DATE ISSUED APR 12 1990
93

ornl

ORNL/TM-11368

ORNL
MASTER COPY

OAK RIDGE
NATIONAL
LABORATORY

MARTIN MARIETTA

Groundwater Parameters and Flow Systems Near Oak Ridge National Laboratory

Gerald K. Moore

Environmental Sciences Division
Publication No. 3403

ChemRisk Document No. 364

NAGED BY
RTIN MARIETTA ENERGY SYSTEMS, INC.
THE UNITED STATES
ARTMENT OF ENERGY

This report has been reproduced directly from the best available copy.

Available to DOE and DOE contractors from the Office of Scientific and Technical Information, P.O. Box 62, Oak Ridge, TN 37831; prices available from (615) 576-8401, FTS 626-8401.

Available to the public from the National Technical Information Service, U.S. Department of Commerce, 5285 Port Royal Rd., Springfield, VA 22161.
NTIS price codes—Printed Copy: A05 Microfiche A01

This report was prepared as an account of work sponsored by an agency of the United States Government. Neither the United States Government nor any agency thereof, nor any of their employees, makes any warranty, express or implied, or assumes any legal liability or responsibility for the accuracy, completeness, or usefulness of any information, apparatus, product, or process disclosed, or represents that its use would not infringe privately owned rights. Reference herein to any specific commercial product, process, or service by trade name, trademark, manufacturer, or otherwise, does not necessarily constitute or imply its endorsement, recommendation, or favoring by the United States Government or any agency thereof. The views and opinions of authors expressed herein do not necessarily state or reflect those of the United States Government or any agency thereof.

ORNL/TM-11368

Environmental Sciences Division

GROUNDWATER PARAMETERS AND FLOW SYSTEMS NEAR OAK RIDGE NATIONAL LABORATORY

Gerald K. Moore
Research Associate, the University of Tennessee, Knoxville

Environmental Sciences Division
Publication No. 3403

Date Published--September 1989

NUCLEAR AND CHEMICAL WASTE PROGRAMS
(Activity No. KG 02 00 00 0; ERKG002)
Office of Energy Research

Prepared by the
OAK RIDGE NATIONAL LABORATORY
Oak Ridge, Tennessee 37831-6285
operated by
MARTIN MARIETTA ENERGY SYSTEMS, INC.
for the
U.S. DEPARTMENT OF ENERGY
under contract DE-AC05-84OR21400

CONTENTS

	Page
LIST OF FIGURES	v
LIST OF TABLES	vii
ABSTRACT	ix
1. INTRODUCTION	1
1.1 BASIC CONCEPTS	3
1.2 HILLSLOPE HYDROLOGY	9
1.3 STATISTICAL DATA ANALYSIS	13
2. HYDROLOGY OF THE STORMFLOW ZONE	15
2.1 POROSITY	15
2.2 PERMEABILITY	16
2.3 WATER INFLOW	21
2.4 LATERAL FLOW	22
2.5 WATER OUTFLOW	25
3. HYDROLOGY OF THE VADOSE ZONE	30
3.1 POROSITY	31
3.2 PERMEABILITY	31
3.3 VERTICAL FLOW AND RECHARGE	33
3.4 WATER BUDGET	37
4. HYDROLOGY OF THE SHALLOW AQUIFER	41
4.1 PERMEABILITY AND HYDRAULICS	42
4.2 FRACTURE CHARACTERISTICS	50
4.3 FLOW RATE	55
4.4 PATH LENGTH	57
4.5 WATER DISCHARGE	58
5. HYDROLOGY OF THE DEEPER AQUIFER	64
6. APPROACH TO MODELING	67
7. FUTURE RESEARCH	69
8. CONCLUSIONS	72
REFERENCES	77

LIST OF FIGURES

Figure		Page
1	Locations of Waste Area Groupings (WAGs) and ORNL study area (the area north of the Clinch River and including the WAGs). .	2
2	Section showing subsurface zones and directions of groundwater flow	5
3	Theoretical changes in hydrography during periods of precipitation and increasing stormflow, showing increases in drainage density and numbers of source areas	12
4	Cumulative probability graph of hydraulic conductivity data obtained from infiltration tests in forested areas	17
5	Cumulative probability graph of merged hydraulic conductivity data from infiltration tests in the stormflow and vadose zones	19
6	Estimated average values of hydraulic conductivity in the stormflow zone at various depths and saturated thicknesses . .	20
7	Cumulative probability graph of hydraulic conductivity data obtained from infiltrometer tests in the vadose zone	32
8	Selected water level hydrographs for observation wells (located in WAGs 3 and 5) and precipitation for the 1986 water year	34
9	Observation wells where water levels reach depths of less than 1.5 m (crosses) and more than 9 m (squares).	40
10	Cumulative probability graph of merged hydraulic conductivity data fro water-producing intervals and matrix fractures. . . .	43
11	Cumulative probability graph of hydraulic conductivity data for water-producing intervals.	44
12	Cumulative probability graph of hydraulic conductivity values for matrix fractures	46
13	Relationship between hydraulic conductivity and transmissivity/hydraulic conductivity ratio values	49
14	Sections showing hypothetical differences in trend and densities of fractures near ORNL	53

LIST OF TABLES

Table		Page
1	Statistical summary of important constituents and properties in water from the shallow aquifer (Specific conductance in micromhos/cm at 25°C, alkalinity as mg/L of $CaCO_3$, and other units, except pH, in mg/L)	8

ABSTRACT

MOORE, G. K. 1989. Groundwater parameters and flow systems near Oak Ridge National Laboratory. ORNL/TM-11368. Oak Ridge National Laboratory, Oak Ridge, Tennessee. 93 pp.

Precipitation near Oak Ridge National Laboratory (ORNL) averages 132 cm/yr. About 76 cm/yr of water is consumed by evapotranspiration. The natural streamflow, which averages 56 cm/yr of water, consists of overland flow (about 21 cm/yr) from water bodies, wetlands, and impervious areas and of groundwater discharge (about 35 cm/yr of water). Groundwater occurs in a stormflow zone that extends from the land surface to a depth of 0.3-2 m and in shallow and deeper aquifers that extend from the water table to the base of fresh water. In the stormflow zone, most water flows through macropores and mesopores, which have a volumetric porosity of about 0.002. In the vadose zone and below the water table, water flows through fractures that have a volumetric porosity in the range 1×10^{-5} to 0.02.

Water inflow occurs by precipitation and infiltration. Infiltration that exceeds the soil water deficit forms a perched water table in the stormflow zone at the level where infiltration rate exceeds vertical hydraulic conductivity. Some water percolates down to the water table but the majority flows downslope to the streams. Recharge of the shallow aquifer is only about 3.2 cm/yr of water or 5.7% of streamflow. Most of the water that recharges the shallow aquifer is discharged by evapotranspiration above the water table. The remainder is discharged at springs and streams where the water table is within the stormflow zone. Digital models that permit unsaturated conditions and transient flows may be more appropriate than steady-state models of saturated flow for the ORNL area.

1. INTRODUCTION

This report is intended to supplement a recent study (Moore 1988) that revised the concepts of groundwater occurrence and flow in the Oak Ridge National Laboratory (ORNL) area (Fig. 1). Some new data have been acquired, but the present report, for the most part, consists of a further interpretation of previously available data. Several additional factors and processes that may affect the groundwater budget of the ORNL area are described. Also, some parameter values in the previous report were based on relatively few data; the present report uses convergence of evidence to test these values. Finally, the additional interpretations in the present report revise some of the parameter values (such as amounts and rates of recharge) in the previous report. The purposes of the present report are to derive more accurate parameter values for future digital modeling and to better characterize the various groundwater flow systems. The resulting conceptual model should be applicable to other areas on the Oak Ridge Reservation and to many other areas underlain by consolidated rocks.

The main problem resulting from the storage of radioactive and mixed wastes in shallow burial grounds near ORNL and from accidental leaks and spills has been the mobility of contaminants in groundwater and the surface discharge of these contaminants at sumps, seeps, and springs. Remedial investigation and action to correct these problems were intensified as a part of the Environmental Restoration and Facilities Upgrade (ERFU) program, begun at ORNL in FY 1986. The program plan includes acquisition of basic geologic and hydrologic data followed by a determination of geochemical

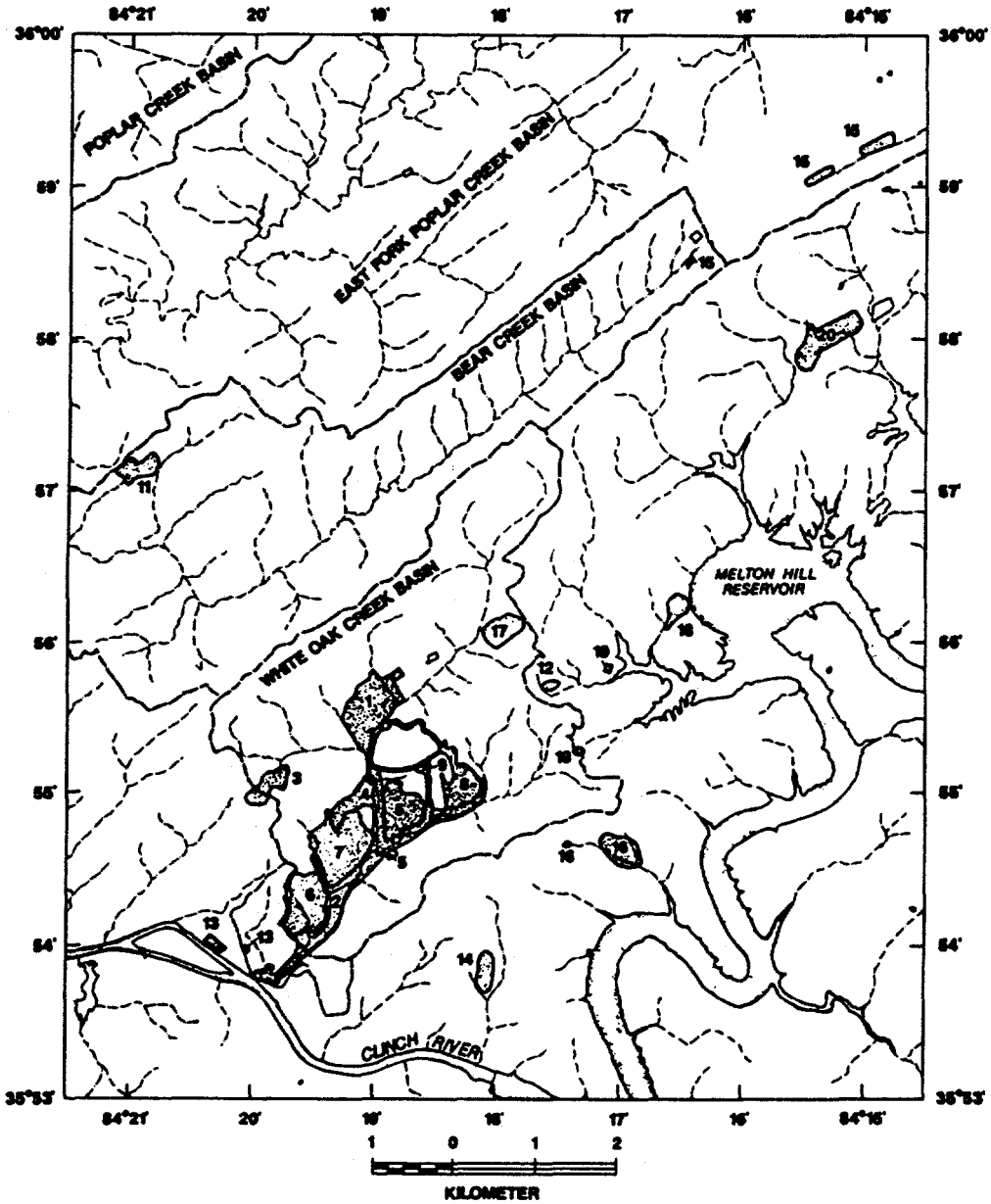

Fig. 1. Locations of Waste Area Groupings (WAGs) and ORNL study area (the area north of the Clinch River and including the WAGs).

processes and by identification and modeling of pathways and contaminant migration. The strategy includes determining the limits of the uppermost aquifer as specified by the U.S. Environmental Protection Agency (U.S. EPA 1986) under the Resource Conservation and Recovery Act (RCRA).

Most of the groundwater objectives of the ERFU Program have been achieved. The drilling and testing of new piezometer, hydrostatic head, and water quality wells have resulted in new concepts of groundwater occurrence and flow (Moore 1988) that explain contaminant migration and discharge; these concepts are important because remedial action may prove to be simpler and less expensive than was previously believed. Also, the understanding of groundwater processes and flow systems in the ORNL area is now adequate to begin the selection, calibration, and verification of digital models.

1.1 BASIC CONCEPTS

The land surface is very permeable in the ORNL area, and nearly all precipitation (an average 132 cm/yr) infiltrates. Exceptions occur in a few areas with urban features, wetlands, water bodies, and barren lands. The majority of the infiltration (76 cm/yr) replenishes soil water within the root zone of vegetation and is later consumed by evapotranspiration. A majority of the remaining water (56 cm in an average year) moves through the ground to discharge locations at nearby seeps, springs, and streams. Most springs are wet-weather types, and, one by one, these springs cease to flow during periods of dry weather. Thus, most groundwater discharge ceases after a few days to weeks of dry weather, and changes in streamflow are

accompanied by changes in the total length of flowing channels.

Groundwater occurs in a stormflow zone that extends from the land surface to a depth of about 0.3-2 m and in shallow and deeper aquifers that extend from the water table to the base of fresh water (Fig. 2). The stormflow zone may be formed by the roots of vegetation. It is thicker and more permeable in forested areas than in grassy and brushy areas; it also is much more permeable at the land surface than at deeper levels. The dominant openings for groundwater flow in this zone are macropores and mesopores (openings larger than 0.03 mm).

The upper part of the stormflow zone is an average of about 1000 times more permeable than the underlying vadose zone, and a majority of all groundwater flow occurs in the stormflow zone. The downward percolation of water from precipitation and infiltration proceeds to less permeable levels and causes perched water. Most groundwater then moves laterally through the stormflow zone toward the streams; a small remainder percolates down, through the vadose zone, to the water table. The perched water table and the resulting lateral groundwater flow are transient beneath the hills but are nearly perennial at valley edges. The decrease in permeability of the stormflow zone with depth means that a small increase in the saturated thickness of the stormflow zone produces a large increase in average permeability. The rates of groundwater discharge to streams change by more than two orders of magnitude during an average year. Based on relatively few data, water in the stormflow zone is acidic to nearly neutral and is a calcium bicarbonate type. The water typically has smaller but significant concentrations of magnesium, sodium, and sulfate. The content of total

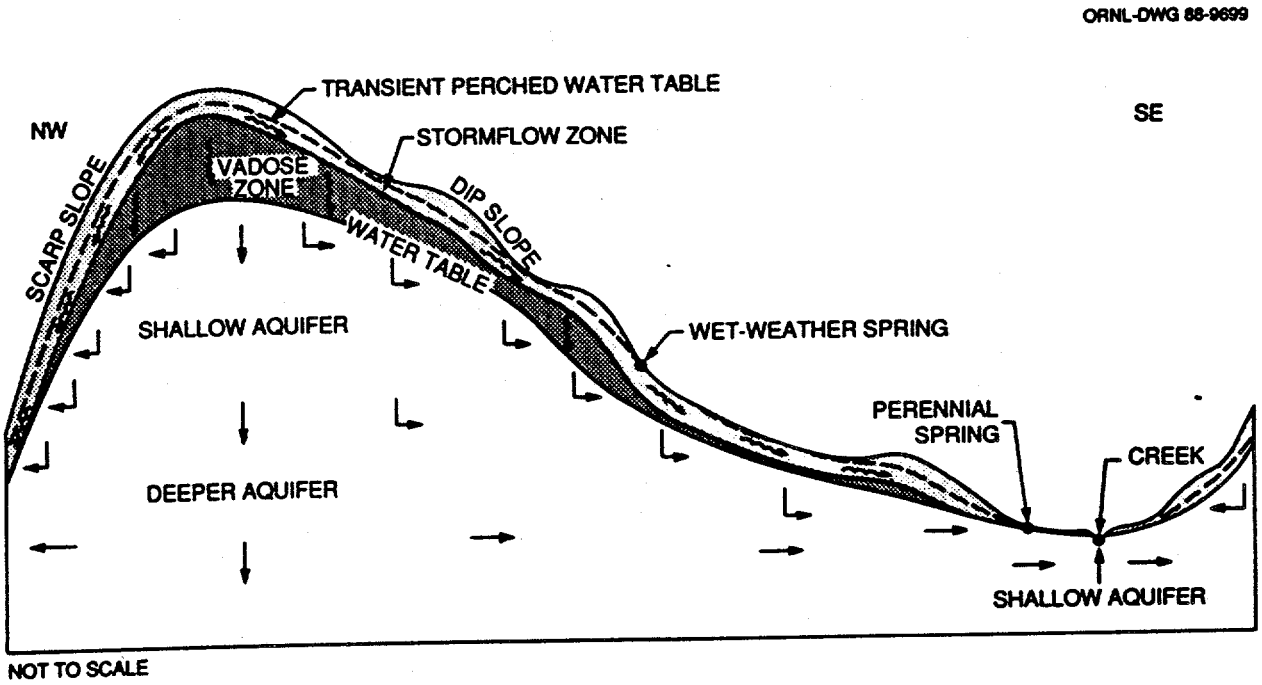

Fig. 2. Section showing subsurface zones and directions of groundwater flow.

dissolved solids is less than 100 mg/L.

A thin vadose zone generally separates the stormflow zone and the shallow aquifer, but the water table is within the stormflow zone near discharge locations. The openings for groundwater flow in the vadose zone are fractures and a few cavities. Most flow paths are near vertical, but lateral velocities of 20-200 m/d occur in a few cavities above or at the water table. Cavities of this type occur only where the water table is within a limestone or dolostone bedrock.

The openings for groundwater flow below the water table are fractures and cavities. Water-bearing fractures are ubiquitous below the water table, but enlarged fractures and cavities are common only at shallow depths. These enlarged openings are the targets for wells and constitute the water-producing intervals in wells. The geometric mean of hydraulic conductivity for the water-producing intervals is about 100 times larger than for other intervals and deeper levels. The shallow aquifer (Fig. 2) generally consists of several water-producing intervals in otherwise relatively impermeable material. In areas underlain by the Conasauga and Chickamauga groups, the shallow aquifer extends to a depth of 20-30 m. In the Knox Group, enlarged openings are common at depths of 30-60 m, and one cavity was reported at a depth of 96 m.

Groundwater is unconfined near the water table, but there is a gradual change to confined conditions at deeper levels. Flowing wells occur in a few areas, and water levels in some of the deeper wells respond to earth tides and other loading forces. Cavities occur in all units that have limy layers but are more common in the Knox Group. Both the lateral and vertical

spatial frequency of cavity occurrence are about four times larger in the Knox Group than in the Rome Formation, the Conasauga Group, and the Chickamauga Group. Based on relatively few data, cavities below the water table have a geometric mean of hydraulic conductivity that is not significantly larger than that of other water-producing intervals.

Flow paths in the shallow aquifer may be nearly linear or complex. Along a single fracture, groundwater may flow downdip and laterally in either or both of two directions. Changes in flow direction are possible at fracture intersections, as are splits and joins of the flow paths. Multiple flow paths connect any two points in the aquifer, and a contaminant introduced at one point in the aquifer may eventually occur in all fractures within a semicylindrical volume of the aquifer. Flow paths generally trend toward lower elevations, and groundwater in the shallow aquifer flows into the stormflow zone near the streams. On hillsides, lateral flows of groundwater may also be discharged by transpiration wherever the water table is less than 2-3 m below land surface.

Groundwater in the shallow aquifer generally is neutral to moderately alkaline and a calcium bicarbonate type (Table 1). Based on a correlation with specific conductance, the geometric mean content of total dissolved solids is 204 mg/L, and the range from the mean minus one to plus one standard deviation is 93-414 mg/L. The concentrations of chemical constituents in groundwater are not spatially correlated and are not constant through time. Nearby wells may have large differences in the specific conductance of water, for example, and monthly changes of more than 60% in specific conductance have been measured. Shallow wells generally

Table 1. Statistical summary of important constituents and properties in water from the shallow aquifer (Specific conductance in micromhos/cm at 25°C, alkalinity as mg/L of $CaCO_3$, and other units, except pH, in mg/L)

Constituent or property	Number of values	Mean[a]	Mean minus one standard deviation	Mean plus one standard deviation	Minimum value	Maximum value
Specific conductance	138	400	220	740	110	1930
pH	133	7.3	6.7	7.9	6.2	9.2
Calcium	187	91	38	220	12	1600
Magnesium	183	12	6.2	24	2.1	137
Sodium	198	14	4.1	45	0.7	420
Alkalinity	126	230	140	370	55	847
Sulfate	162	22	9.5	54	4.0	376
Chloride	167	7.9	2.4	27	0	200

[a]Arithmetic mean for pH; geometric mean for others.

have a smaller and more variable specific conductance of water than deep wells, but other relationships are also common.

Only a small percentage of the groundwater follows flow paths through the deeper aquifer. This water eventually flows upward, back into the shallow aquifer, near discharge locations. Brine, which probably is connate, occurs at depths below about 150 m in Melton Valley, and this is the approximate base of the deeper aquifer. Elsewhere, however, the base of fresh water has not been determined.

1.2 HILLSLOPE HYDROLOGY

The relative importance of the stormflow zone to the hydrology and water budget of the study area is not a new concept. As early as 1932, C. R. Hursh[1] concluded that virtually all precipitation infiltrates the soil in forested areas of the eastern United States. In the 1940's, Hursh and his colleagues at the Coweeta research laboratory of U.S. Forest Service recognized both rapid and delayed responses of streamflow to precipitation as well as changes in headwater locations and differences in the responses of headwater tributaries and downstream reaches. Detailed studies of Coweeta hydrology by J. D. Hewlett, A. R. Hibbert, and others in the 1960's resulted in many concepts of hillslope hydrology that are generally accepted today. In the ORNL area, recent studies at the Walker Branch watershed have

---

[1] A history of research at the Coweeta Hydrologic Laboratory in Otto, North Carolina and the original references are included in Swank and Crossley (1988, pp. 46-55, 111-127).

documented lateral flows in B-horizon soils at depth of about 15-140 cm during winter storms (G. V. Wilson, P. M. Jardine, R. J. Luxmoore, et al., ORNL, written communication, 1989).

During periods of rain in the ORNL area, the initial increase in streamflow results from precipitation on stream channels and adjacent wetlands. Soon afterwards, waters from storm-drain systems, impervious areas, and more distant wetlands contribute to increasing streamflows. These responses are more prominent at downstream locations than at headwater tributaries, apparently because subsurface stormflow processes dominate the streamflow hydrograph in most headwater areas. For small amounts of precipitation, especially during the growing season, channel interception and other types of overland runoff are the dominant sources of increased streamflow. For larger amounts of precipitation during dry periods, however, and for precipitation during the wet winter months, most streamflow increases are produced by groundwater discharge from the stormflow zone. Stormflow discharge is larger along headwater tributaries than along downstream reaches because of convergent flows, as is discussed below. After prolonged or intense periods of rain, streams may also receive overland runoff from grassy and sodded areas (temporary wetlands) where the stormflow zone may have less capacity for water storage than in forested areas. Depression water storage is commonly observed over a large part of bottomland pastures following intense storms.

Groundwater flow paths converge in all valley areas that have concave slopes above the emergent source of a flowing tributary whereas flow paths are nearly linear toward any flowing channel farther downstream. With

continued precipitation, the converging flows eventually fill the stormflow zone to overflowing, thereby forming wet-weather springs, source areas for streamflow, and flowing tributary streams below these locations (Fig. 3). The source areas expand rapidly at first, and the saturated soils contribute to overland sheet flow by both groundwater discharge and precipitation interception. However, channel flow soon begins, and the source area then shrinks as flow paths toward these channels become linear.

Factors and conditions that favor an early appearance of a source area are a location where the stormflow zone is nearly filled with water, a thin but permeable material, a steep hydraulic gradient, and a location where groundwater flow paths from several side slopes converge. The relative importance of these factors in the study area has not been determined, but source areas appear early at low elevations and later at locations progressively closer to the drainage divides (Fig. 3). This observation suggests that having a stormflow zone nearly filled by previous drainage from higher elevations is the most important condition; the other factors contribute to this condition. When precipitation ends and streamflow decreases, the process reverses; one by one, source areas decrease in size, and wet-weather springs cease to flow, as do the downstream tributary channels.

Between precipitation events, water drains from the stormflow and vadose zones, and the discharge of this water supports the decreasing base flow of the streams. Physical models, digital models, and other research at Coweeta Hydrologic Laboratory have shown that all base streamflow can probably be explained by this drainage and that any contributions from

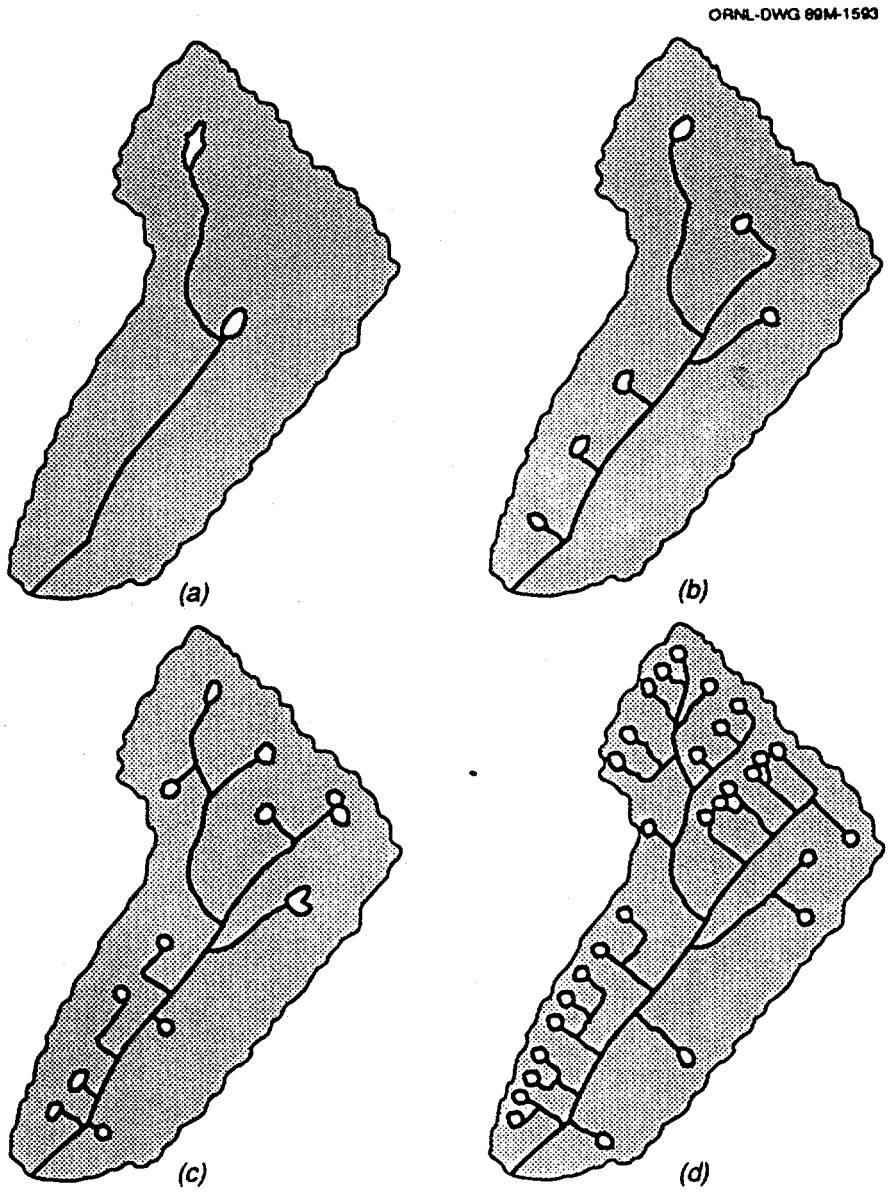

Fig. 3. Theoretical changes in hydrography during periods of precipitation and increasing stormflow, showing increases in drainage density and numbers of source areas (after Hewlett and Nutter 1970).

fractured rocks below the water table are minor to insignificant. In the ORNL study area, however, the water table is within the stormflow zone near the streams. Because of this condition and the possible lateral flow of water from the shallow aquifer into the stormflow zone at higher elevations (as is discussed later), the relative importance of the stormflow zone as the water source for base streamflow cannot easily be determined. The chemical content of base streamflow in the ORNL area indicates that water from the shallow aquifer is an important component of this flow.

1.3 STATISTICAL DATA ANALYSIS

Groundwater parameters in the study area have a large numeric range, little correlation with other parameters, and abrupt spatial changes in value. Tools such as contour maps and regression analyses have limited utility in this area and can produce misleading results. The problem apparently results from nearly unique conditions along each of the many groundwater flow paths. In this situation, statistical analysis may be the best approach to parameter characterization. Cumulative probability graphs are used for analysis of parameter values in this report. These graphs require a fairly large amount of data but may show sample or population characteristics that otherwise would be obscure. Some deviations on cumulative probability graphs represent only an imperfect distribution of sample values, but others show a change in conditions at deeper levels in the aquifers or show some type of control on the range of parameter values. A correct interpretation of the significant deviations can contribute to an

understanding of groundwater occurrence and flow paths.

The construction and use of probability graphs for analysis of geoscience data are fully described by Sinclair (1976). Basically the method consists of plotting sorted data values on cumulative probability paper; the data points are those that would be used for a cumulative histogram. If a straight line can be fitted to the data points, this line defines the cumulative normal density distribution of the population. A Gaussian population plots as a straight line on arithmetic probability paper, and a lognormal population plots as a straight line on logarithmic probability paper. The 50 percentile value of the line represents the arithmetic mean of a normal population and the geometric mean of a lognormal population. Similarly, values for the mean minus or plus one standard deviation can be read from the 16 and 84 percentile values of the line.

In the study area, all hydrologic parameters that were plotted on probability paper were lognormally distributed, but some parameters had a much larger data range than did others. Parameters with a relatively small range were plotted on a logarithmic scale whereas the natural logarithms of other parameter values were plotted on an arithmetic scale. Graphically, both methods produce the same result. In the latter case, however, values such as the geometric mean must be calculated from $\underline{e}^{x}$, where $\underline{x}$ is the value determined from the line.

Probability graphs provide a simple procedure for determining the type of distribution and for detecting abnormalities in the sample. The disadvantages of probability graphs include the need for a fairly large amount of data and the possibility of an erroneous interpretation.

2. HYDROLOGY OF THE STORMFLOW ZONE

The stormflow zone extends from the land surface to a depth of 0.3–2 m; it may have an average thickness of about 1.2 m in forested areas and 0.8 m in sodded areas. The important hydrologic parameters of this zone are the capacity for water storage, the saturated thickness, and the average permeability of the saturated interval. Water storage in the stormflow zone is nearly all intergranular, but the openings for lateral flow are macropores and mesopores. The porosity of clay soils is generally about 50%. However, Watson and Luxmoore (1986, p. 581) found that macropores and mesopores, which together occupy only 0.2% of the soil volume, account for 96% of the infiltration. Macropores and mesopores are not completely understood but are connected voids that may have various causes, including biochanneling, cracking, and aggregation of soil particles. Water is added to the stormflow zone by the infiltration of precipitation and by lateral flow from other zones. Water is removed by evapotranspiration, discharge to springs and streams, and downward percolation through the vadose zone.

2.1 POROSITY

The estimated 50% porosity of the clayey stormflow zone represents the total water storage capacity of this layer, but only a part of the stored water contributes to hydrologic processes. The field capacity of a clay is commonly about 40% (Bouwer 1978, pp. 260–261); about 10% of the saturated material is water that will drain under the influence of gravity. Soil

water content at the wilting point of vegetation is about 30% for a clay soil (Bouwer 1978, p. 265); an additional 10% of the soil volume in the root zone is water that is available for transpiration. Soil water contents below 30% are possible by surface evaporation, but vegetation wilting is uncommon in the study area. A typical water content in the stormflow zone may range from 30% to 50% of soil volume; the soil water deficit thus ranges from 0.1-0.2 and may average about 0.15. If so, the total storage capacity of the stormflow zone is about 18 cm of water in forest areas and 12 cm of water in sod areas. The effective porosity for vertical and lateral flows through macropores and mesopores, however, is only about 0.002.

2.2 PERMEABILITY

A cumulative probability graph of permeability data from infiltration tests on forest soils (Watson and Luxmoore 1986; Wilson and Luxmoore 1988) shows a lognormal distribution (Fig. 4). The geometric mean infiltration rate is 8.8 m/d, and the range from the mean minus one to the mean plus one standard deviation is 3.2-23 m/d. One-hour precipitation intensity does not exceed 1.9 m/d in the study area (McMaster 1967, p. 8). These data show that virtually all precipitation is readily absorbed by forest soils. Infiltration tests have not been made in grassy, sedgy, and brushy areas, but evidence of overland flow (lodged vegetation and matted detritus) is rarely observed in these areas. Average infiltration rate is apparently larger than precipitation intensity during storms.

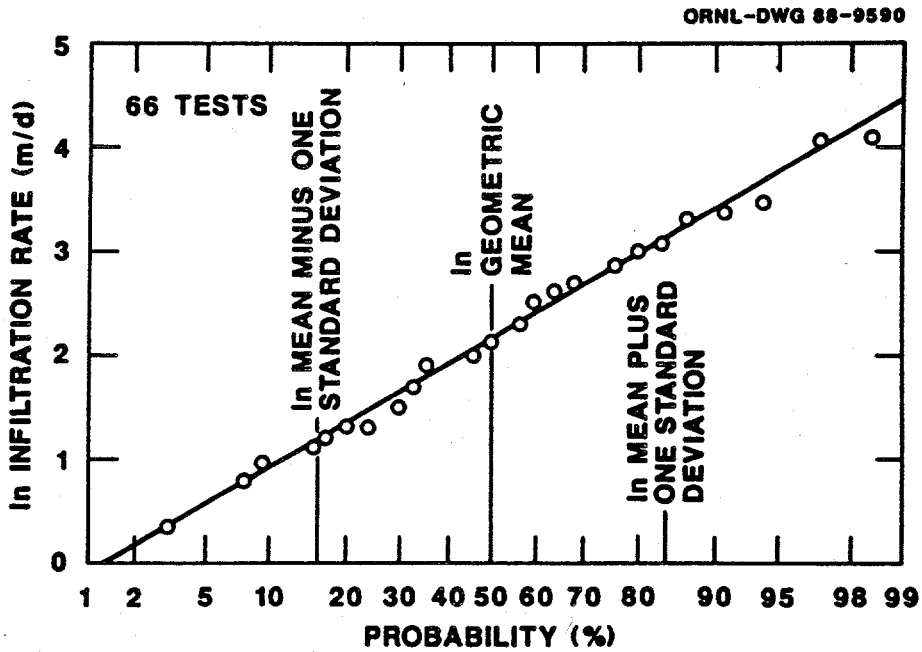

Fig. 4. Cumulative probability graph of hydraulic conductivity data obtained from infiltration tests in forested areas.

Other infiltration tests were made in areas where A- and B-horizon soils had been removed (Luxmoore et al. 1981, p. 688; Davis et al. 1984, p. 72) and at shallow depths in boreholes on Chestnut Ridge (summarized in Ketelle and Huff 1984, pp. 75-77). A cumulative probability graph of the merged data (Fig. 5) shows two slopes, thereby indicating two different populations. The upper population is assumed to represent permeabilities near the base of the stormflow zone; the geometric mean of hydraulic conductivity is 0.032 m/d. The lower population is assumed to represent permeabilities in the underlying vadose zone; the geometric mean of hydraulic conductivity for this population is 0.0019 m/d. The minimum hydraulic conductivity in the upper population is the same as the maximum value in the lower population and is 0.011 m/d.

The average hydraulic conductivity of the stormflow zone apparently decreases with depth. Bouwer (1978, p. 264) noted that roots are concentrated in the upper layer of soil for all types of vegetation, and Kirkby (1988, p. 319) stated that both vertical hydraulic conductivity and porosity typically decrease at depth. The form of the distribution of hydraulic conductivity values with depth is unknown but is relatively unimportant for the estimates that follow. The infiltration tests in forested areas were made at a depth of about 15 cm (Watson and Luxmoore 1986, p. 578), and the subsoil permeability data can be assumed to represent the base of the stormflow zone at a depth of 120 cm. If these two points are plotted on a graph and are connected by a straight line (Fig. 6), estimates of average hydraulic conductivities at other depths can be

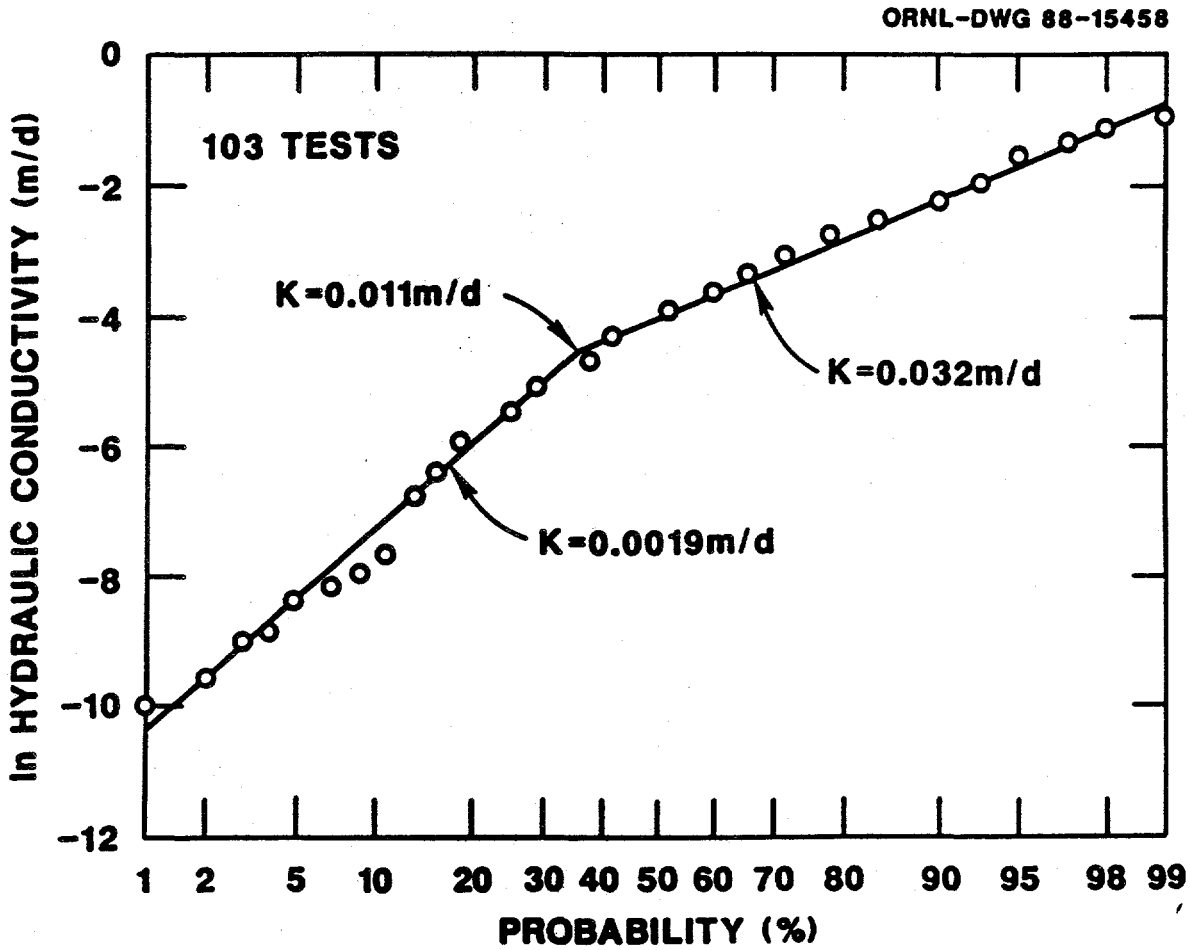

Fig. 5. Cumulative probability graph of merged hydraulic conductivity data from infiltration tests in the stormflow and vadose zones.

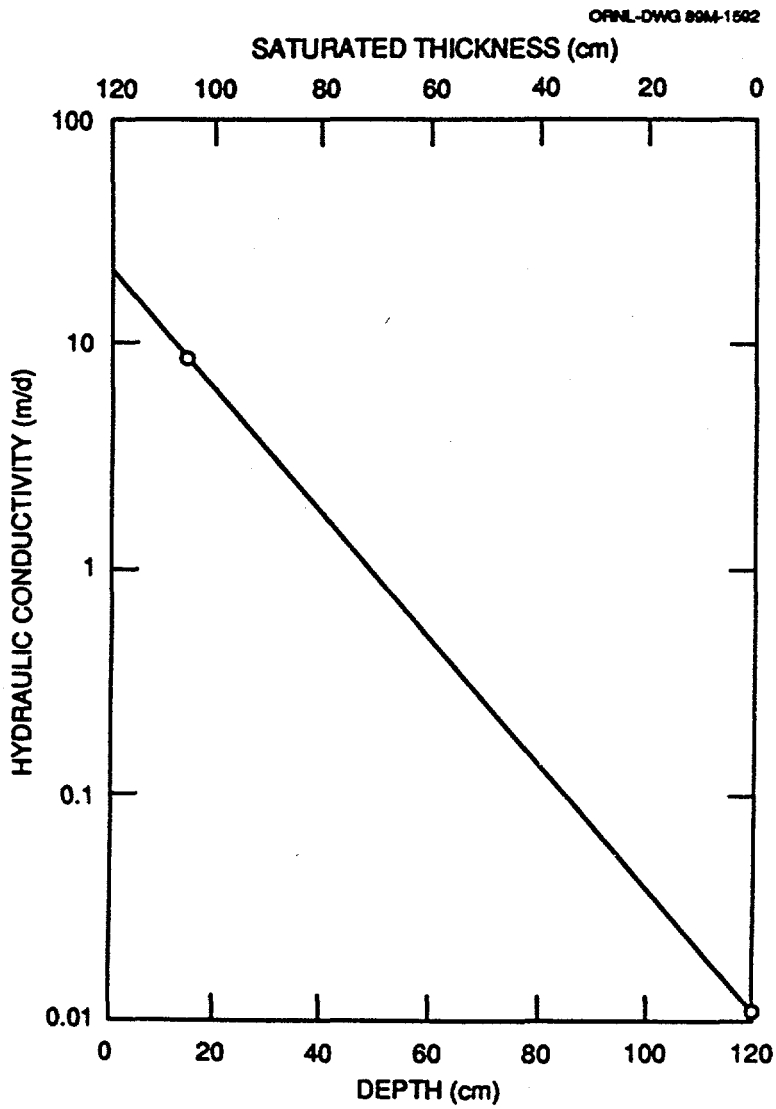

Fig. 6. Estimated average values of hydraulic conductivity in the stormflow zone at various depths and saturated thicknesses

obtained from the line. This line is speculative, but it can be used to estimate vertical and lateral flow rates.

2.3 WATER INFLOW

The infiltration of water from precipitation is the main source of water in the stormflow zone. This process first replenishes any soil water deficit within the root zone of vegetation. After field capacity has been reached, continued infiltration causes water to move vertically until it reaches a level where the percolation rate exceeds the hydraulic conductivity of the material. Water accumulates above this level and forms a transient perched water table. If the relationship in Fig. 6 is assumed to be correct, an infiltration rate of 2.54 cm/hr (0.61 m/d), for example, would form a perched water table above a depth of about 55 cm. Below the perched water table, vertical percolation continues, but water in the saturated material also flows laterally in the direction of the hydraulic gradient.

The water table is within the stormflow zone near streams, and groundwater from the shallow aquifer moves through the stormflow zone to the streams. Water also might be added to the stormflow zone by lateral flows at higher elevations. The evidence is discussd later, but lateral water flow to the stormflow zone might occur above the water table because of the contrast in permeability between water-producing openings and the surrounding material (the fractured matrix).

2.4 LATERAL FLOW

During dry periods, the lateral downslope movement of water in the stormflow zone means that the saturated thickness of this zone decreases sooner on the ridges than in the valleys. Drainage of material above the perched water table, from saturated conditions to field capacity, probably continues for a period of days to weeks, but vertical percolation through the vadose zone also continues, as does evapotranspiration. Lateral flow of perched water thus is generally transient, a few days to a few weeks after the end of precipitation. Lateral flow continues longer in the valleys than on hills and ridges, and it is perennial in the same lower parts of the basins as flowing streams. It may be perennial farther up the basin, but the groundwater in this area is captured by evapotranspiration before reaching the stream channels. A seepage run (closely spaced measurements of streamflow) by U.S. Geological Survey (USGS) on June 28, 1988, showed that natural streamflow in the White Oak Creek basin was near zero; nearly all of the 165 L/s of streamflow below the confluence of White Oak Creek and Melton Branch was effluent from imported water (H. H. Zehner, USGS, personal communication, 1988). Groundwater flow above the levels of the valley floors continued, as was shown by water level elevations in observation wells. Elsewhere in Tennessee, an increase in streamflow is commonly observed after the first killing frost in the fall.

Average linear velocity of groundwater and both lateral and vertical flow rates can be calculated from forms of Darcy's law:

$$V = -Ki/n, \qquad (1)$$

$$Q_1 = -Ki, \qquad (2)$$

$$Q_2 = -Kiwb, \qquad (3)$$

where $\underline{V}$ is average linear velocity, $\underline{K}$ is hydraulic conductivity, $\underline{i}$ is hydraulic gradient, $\underline{n}$ is volumetric porosity, $\underline{Q_1}$ is flow rate per unit area, $\underline{Q_2}$ is flow rate through a measured cross-sectional area, $\underline{w}$ is width of a rectangular flow tube, and $\underline{b}$ is saturated thickness of a flow tube. The effective hydraulic gradient for lateral flow of water in the stormflow zone is probably the same as surface slope. The maximum slope of the land surface generally is <0.3, although locally, the steepest part of a scarp slope may be >0.5. Surface slope is generally not <0.03 except on the floodplain of the Clinch River, where it may average about 0.015. The average surface slope and hydraulic gradient may be about 0.075 in the ORNL area.

Assume a hydraulic gradient of 0.075 and an average hydraulic conductivity of 8.8 m/d near the top of the stormflow zone and 0.032 m/d near its base. If nearly all flow occurs through macropores and mesopores, the effective porosity is about 0.002. Based on these values, the average linear velocity of lateral water flow (eq. 1) is 300 m/d near the top of the stormflow zone but only 1.2 m/d near its base. These results show that lateral flow toward discharge locations would be rapid whenever and wherever the stormflow zone is full but relatively slow when it is nearly drained.

The diameters of openings in the stormflow zone can be calculated from the Hagen-Poiseuille law for laminar flow in tubes:

$$h = 32vLVg^{-1}D^{-2},$$

where h is head loss, v is the kinematic viscosity of water, L is length of tube, g is acceleration of gravity, and D is tube diameter. In English units at 15°C, this equation can be reduced to:

$$D = (1.35 \times 10^{-5}V/i)^{0.5}.$$

Substituting the equation for velocity in Darcy's law:

$$D = (1.35 \times 10^{-5}K/n)^{0.5}.$$

For D in ft and K in ft/s, the units are correct because of the reduction in terms, above. If flow occurs through macropores and mesopores, the porosity is about 0.002. Assuming that hydraulic conductivity is 8.8 m/d (3.3×10^{-4} ft/s) near the top of the stormflow zone and 0.032 m/d (1.2×10^{-6} ft/s) near its base, the mean diameters of the flow tubes are 0.46 mm near the top of the zone and 0.028 mm near the base of the zone. The average tube size near the base of the zone is approximately the same as the minimum size of mesopores; this result supports the interpretation (Fig. 5) that was used for the construction of Fig. 6.

Assume that the hydraulic conductivities in Fig. 6 are correct and that the average hydraulic gradient is 0.075. Also assume a flow tube 1 m wide. The incremental and cumulative rates of lateral flow in the stormflow zone for saturated depths of 10-120 cm are shown in the data below. The data show that the flow rate in each saturated interval (10 cm thick) is approximately twice as large as that in the underlying interval. Calculations based on Fig. 6 and eq. (3) show that when the stormflow zone

Saturated depth (cm)		Interval flow rate (m^3/yr)	Total flow rate (m^3/yr)
Interval	Total		
110–120	10	0.040	0.04
100–110	20	0.08	0.12
90–100	30	0.14	0.26
80–90	40	0.27	0.56
70–80	50	0.64	1.1
60–70	60	1.0	2.1
50–60	70	1.8	3.9
40–50	80	3.4	7.3
30–40	90	6.6	14
20–30	100	13	27
10–20	110	24	51
0–10	120	44	95

is full, (1) about half of the lateral water flow is in the top 10% of the zone, (2) 98% of the flow is in the top half of the zone, and (3) the average hydraulic conductivity (2.9 m/d) for the total flow occurs at a depth of 32 cm, about one-fourth of the saturated depth. These relationships change when the stormflow zone is partly filled. If the saturated interval is at depths of 80–120 cm, 25% of the total flow is in the top 10% of the saturated interval, 77% of the flow is in the top half, and the average hydraulic conductivity occurs at a depth of 96 cm.

2.5 WATER OUTFLOW

Water is lost from the stormflow zone by evapotranspiration, by discharge to surface water, and by percolation down to the water table. Mean annual evapotranspiration in the study area is about 76 cm of water; a majority of the transpiration loss occurs in the stormflow zone because roots are concentrated near land surface. Potential evapotranspiration near the study area ranges from an average minimum of about 0.04 cm/d in

midwinter to an average maximum of about 0.5 cm/d in midsummer (Tennessee Division of Water Resources 1961, p. 24).

Streamflow constitutes about 56 cm of water in an average year and the quarterly distribution (after McMaster 1967, p. 48) is approximately as follows:

January–March	April–June	July–September	October–December
27.4 cm	12.9 cm	6.2 cm	9.5 cm

Based on the relationship in Fig. 6 and on eq. (3), the average hydraulic conductivity and saturated thickness of the stormflow zone for these amounts of water are as follows:

Quarter	Hydraulic conductivity (m/d)	Saturated thickness (cm)
January–March	0.081	50
April–June	0.047	39
July–September	0.030	29
October–December	0.038	35

It is interesting that only a 21-cm change in average saturated thickness of the stormflow zone can account for all of the variation in mean quarterly streamflow.

Mean daily streamflows can also be explained by stormflow discharge. The 10% duration flow (exceeded an average of 37 d/yr) is about 3200 $m^3d^{-1}km^{-2}$ (3.4 CFS/mi^2) in the study area (McMaster 1967, pp. 19–28) and is mostly groundwater discharge. This streamflow represents 0.32 cm/d of water, an average saturated thickness of 51 cm, and an average hydraulic conductivity (Fig. 6) of 0.084 m/d in the stormflow zone. The 1% duration streamflow (exceeded an average of 3.7 d/yr) is only partly stormflow discharge because overland flow from source areas is important at these times. Nevertheless,

the average 16,000 $m^3d^{-1}km^{-2}$ (17 CFS/mi^2) flow rate represents a saturated thickness of about 78 cm and an average hydraulic conductivity of 0.28 m/d in the stormflow zone. If no overland flow occurred, stormflow discharge could supply all of this water, although path length would be short, as is discussed later.

Vertical percolation rate below the stormflow zone is determined by the hydraulic gradient for gravity flow (1.0) and by the hydraulic conductivity of the vadose zone. The geometric mean of hydraulic conductivity is 0.0019 m/d, and the average rate of vertical percolation may be about 0.008 cm/hr whenever there is perched water in the stormflow zone. In this case, the rate of lateral flow in the stormflow zone would exceed the rate of vertical percolation whenever there is a saturated depth of more than 10 cm.

At discharge locations, the stormflow zone is filled to overflowing. Assuming that the average saturated thickness is 1.2 m, the average hydraulic conductivity is 2.9 m/d, and the hydraulic gradient is 0.075, the discharge rate from a flow tube 1 m wide is 0.26 m^3/d. If these conditions are uniform over a 1 km^2 area and if all streamflow is stormflow discharge, the 50% duration streamflow (McMaster 1967, pp. 19-28), which is about 580 $m^3d^{-1}km^{-2}$, would require 1.1 km of flowing channel (a drainage density of 1.1 km^{-1}); the 10% duration streamflow would require 6.1 km of flowing channel; and the 1% duration streamflow would require 31 km of flowing channel. These calculations show an expanding drainage network with increasing streamflow. In comparison, (1) the drainage density shown by blue lines on a 1:24,000 scale topographic map is 1.8-2.2 km^{-1} in the White

Oak Creek and Bear Creek basins, and (2) a 1:1200 scale map of the Walker Branch watershed shows a drainage density of 4.4 km^{-1}. Subsurface flow paths would be short during the largest streamflows. Average flow path length can be calculated from the ratio:

$$(PL) = 1000/2(DD),$$

where (PL) is length of the flow path in m and (DD) is drainage density in units of km^{-1}. The average length of a stormflow path at the time of the 50% duration streamflow is 455 m. If the 10% and 1% duration streamflows are all stormflow discharge, flow path lengths would be 82 m and 16 m. The latter distance, at least, seems unreasonably short.

At larger streamflows, an increasing percentage of groundwater discharge is probably from source areas. If source areas are assumed to have a circumference of 80 m, total discharge from 25 of these areas is equal to 1 km of channel discharge.

Half or more of the 1% duration streamflow probably is overland runoff, mainly from source areas. Freeze and Cherry (1979, p. 219) state that overland flows occur on less than 10% of the basin area in most cases and commonly occur on 1-3% of the basin area. Contributing area of overland flow can be calculated (Kirkby 1988, p. 332) as the ratio of (peak streamflow)/(peak rainfall intensity). The 1% duration streamflow is equivalent to a flow rate of 0.067 cm/hr of water. The corresponding rainfall intensity is unknown but can be estimated. About 6.0 cm of water are required to fill the stormflow zone from an average saturated thickness of 38 cm to the level of 78 cm, which corresponds to the 1% duration streamflow. The period for a maximum precipitation intensity of this total

amount of water with a recurrence interval of 1 yr is about 9 hr (McMaster 1967, p. 8). The peak rainfall intensity thus is about 0.67 cm/hr, and the contributing area of overland flow is about 10% of the basin area. A similar calculation for the 10% duration streamflow indicates a contributing area of 0.2% of the basin. These results are unrealistic, however, because the calculations inherently assume that contributing areas and the resulting overland flows produce all streamflow.

It may be reasonable to assume that overland flow constitutes about 20% of the 10% duration streamflow and 70% of the 1% duration streamflow. It may also be reasonable to assume that the number of source areas in 1 km^2 of drainage area increases from 1 at the time of 50% duration streamflow to 9 at the 10% duration streamflow and to 25 at the 1% duration streamflow. If so, the nine source areas at a time of 10% duration streamflow represent the equivalent of about 0.36 km of channel flow; the drainage density at this time is 4.6 km^{-1}; the total length of the new channel is 3.5 km; the average length of each new channel below a new source area is 0.43 km; and the average subsurface path length in the stormflow zone is 110 m. At the time of a 1% duration streamflow, similarly, the 25 source areas represent the equivalent of 1 km of channel discharge; the drainage density at this time is 8.2 km^{-1}; total length of new channel is 3.7 km; average length of each new channel below a new source area is 0.23 km; and average subsurface path length is 61 m. These results, although speculative, are based on the best available data and reasonable assumptions.

3. HYDROLOGY OF THE VADOSE ZONE

A vadose zone occurs between the stormflow zone and the shallow aquifer in most of the study area. The base of the stormflow zone occurs at a depth of about 0.3-2 m. The geometric mean depth of the October water table in the Conasauga Group and the Chickamauga Group is 4.1 m, and the range from the mean minus one to plus one standard deviation is 1.7-10 m (Moore 1988, p. 69). The material in most of the vadose zone is regolith. The geometric mean of regolith thickness is 3.9 m, and the range from the mean minus one to plus one standard deviation is 2.0-7.3 m (Moore 1988, p. 19).

The reason for a water table near the top of bedrock is not completely understood, but the coincidence is probably caused by a porosity change at the base of the regolith. An average depth to water that is slightly larger than the average regolith thickness is probably not important because of the occurrence of a capillary fringe and because of the seasonal fluctuation of the water table.

The vadose zone is unsaturated except in the capillary fringe above the water table and except within wetting fronts during periods of vertical percolation from the stormflow zone to the water table. The important hydrologic parameters of the vadose zone are permeability, capacity for transient water storage, and rates of water drainage. Water is added to the vadose zone by percolation from the stormflow zone; water is removed by transpiration and by recharge of the shallow aquifer. In addition, lateral water flow may occur above the water table through enlarged fractures and a few cavities. The occurrence of cavities in the vadose zone and results of

two tracer tests in cavities are summarized in Moore (1988, pp. 42, 65-66); cavities of this type apparently are rare and are not discussed further in the present report. The other evidence for lateral groundwater flow above the water table is described later.

3.1 POROSITY

Water storage is intergranular in B-horizon and some C-horizon soils but is restricted to fractures in bedrock. An intermediate type of storage may occur in saprolite. The fractional volume that is available for temporary water storage may be in the range 0.10-0.15 for granular regolith, 1×10^{-3} to 0.1 for saprolite, and 1×10^{-5} to 1×10^{-3} for bedrock. Porosity values larger than 1×10^{-3} probably represent some intergranular contributions to water storage. The effective porosity for vertical drainage probably is about the same as water storage capacity in saprolite and bedrock.

3.2 PERMEABILITY

A cumulative probability graph of merged data from infiltrometer tests (Fig. 5) shows that the geometric mean of hydraulic conductivity for the vadose zone is 0.0019 m/d. This value may be slightly more accurate than that obtained from a separate probability graph of 38 infiltrometer tests in the vadose zone (Fig. 7). In the latter graph, the geometric mean of hydraulic conductivity is 0.0030 m/d, and the range from the mean minus one

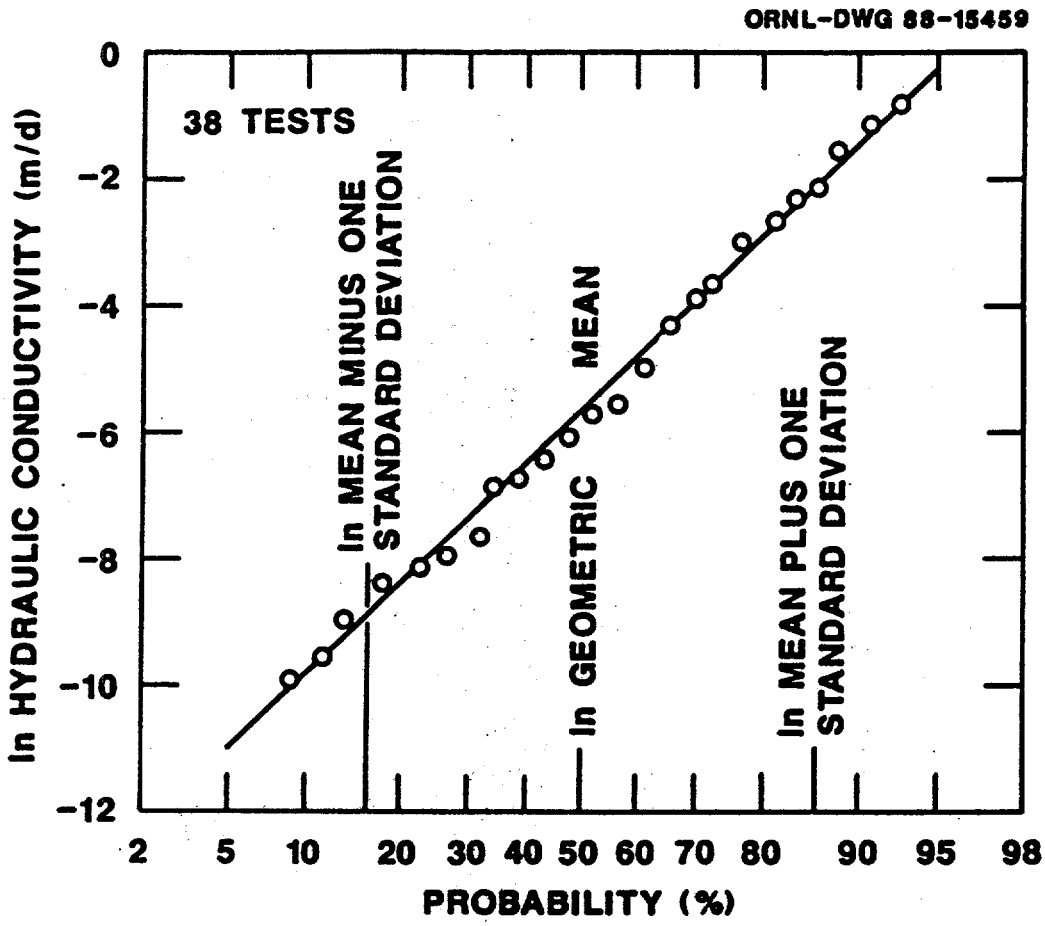

Fig. 7. Cumulative probability graph of hydraulic conductivity data obtained from infiltrometer tests in the vadose zone.

to the mean plus one standard deviation is 1.5×10^{-4} to 0.061 m/d. These values represent saturated conditions, and hydraulic conductivity decreases from a maximum at saturation to nearly zero at field capacity (Freeze and Cherry 1979, pp. 41-44). In addition, as is discussed later, water level fluctuations in wells indicate that local rates and periods of recharge are controlled by the largest openings at some locations and times. At other locations or times recharge is controlled by the smaller pores or by several different types and sizes of openings. The vadose zone thus has both spatial and temporal differences in permeability. Capillary rises to replace water lost to transpiration, which is discussed later, may also cause upward as well as downward water flows. These factors and differences in effective volumetric porosity complicate any calculations of net flow rate and water velocity in the vadose zone.

3.3 VERTICAL FLOW AND RECHARGE

The daily water level hydrographs of 40 observation wells (Fig. 8, for example) maintained by USGS show 1-15 recharge events in the period from midOctober 1985 to midApril 1986. These differences indicate that recharge reaches the water table relatively quickly in areas where water level rises are separated by periods of water level recession. In other areas, separate periods of precipitation and infiltration merge to produce a single recharge event that lasts for a longer period. In the extreme case (represented by 10% of the wells) recharge continued from the beginning of the seasonal rise in water level until the peak.

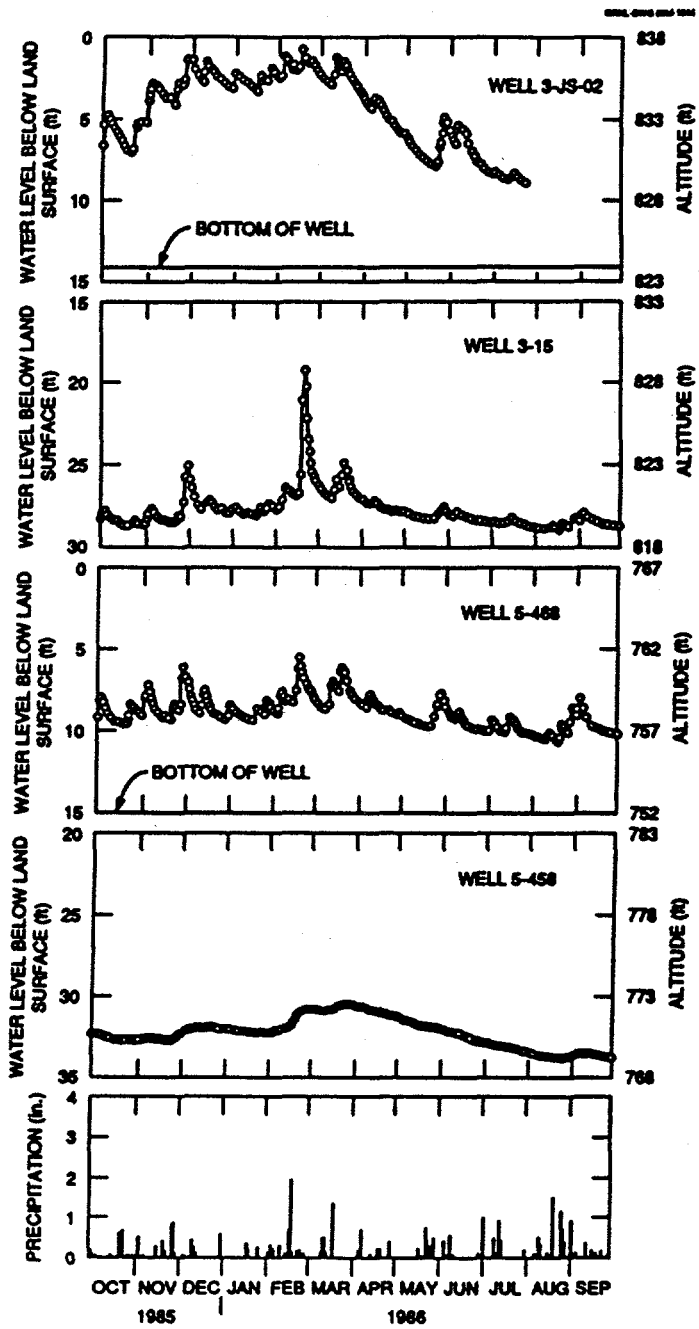

Fig. 8. Selected water level hydrographs for observation wells (located in WAGs 3 and 5) and precipitation for the 1986 water year.

Differences in the times and lengths of recharge periods are also shown by the times of seasonal high and low water levels. Some of the 40 observation wells reached a seasonal low water level on October 20, 1985, and then began a sequence of water level rises. However, the water levels in other wells continued slow declines until October 31, November 10, November 28, and December 15, 1985. Later, most wells recorded a seasonal high water level within 1-4 d after a period of intense precipitation on February 16, 1986. However, some wells did not record a peak water level from this storm until February 28, almost 12 d later. In four wells, water levels continued to rise, past the time of a less intense storm on March 18 to peak levels on March 25, April 1, and May 10, 1986. These results show that recharge begins soon after precipitation in some areas but is delayed for periods of up to 45 d in other areas. Recharge is nearly ended after a period of 1-4 d in some areas but continues for more than 30 d in other areas.

The maximum daily water level rise in response to recharge is 1-10 cm in some of the USGS observation wells but is 30-200 cm in other wells. The smaller amounts of rise are typical of many wells in the Conasauga Group, and the larger amounts are common for wells in the Chickamauga Group. Many of the wells that have rapid rises in water level as a result of precipitation and recharge also have steep rates of water level recession in the absence of recharge. These hydrograph spikes do not represent large changes in aquifer discharge because even the largest changes in water level represent only small changes in hydraulic gradient. Instead, the spike recessions probably indicate water seepage from fractures and macropores

into smaller matrix pores near the water table. The part of the change in water table elevation that affects aquifer discharge rates might be represented by drawing a line to connect the shallower slopes between hydrograph spikes. These base-level lines have the same configuration for wells in both the Conasauga Group and the Chickamauga Group.

A conceptual model of flow in the vadose zone should explain rapid and delayed responses of the water table to precipitation, differences in recharge rates, and both short and prolonged periods of recharge. Because the geometric mean of water table depth is 4.1 m and because the time delay for a water table peak after the end of precipitation is about 1-45 d, the average linear velocity of water in the vadose zone has a range of at least 0.091-4.1 m/d. The actual range for average linear velocity in the vadose zone may be about 0.02-50 m/d because the range in water table depth is about 0.5-18 m and because recharge begins only a few hours after precipitation in some areas.

If the range in average linear velocity for vertical flow is 0.02-50 m/d and is caused by the 10-90% probability values of hydraulic conductivity (Fig. 7; 5×10^{-5} to 0.30 m/d), effective porosity near the water table has a 10-90% probability range of 0.0025-0.0060, and the average value may be about 0.0042. This result is reasonable because it is in the lower part of the possible range for saprolite. The calculated results show that the times and periods of recharge can be explained by the distribution of hydraulic conductivity values in the vadose zone.

The total amount of water level rise during any recharge period is probably explained by the saturated thickness of the wetting front. The

factors that determine saturated thickness are (1) presence of perched water in the stormflow zone for a period of days or weeks, (2) a larger hydraulic conductivity in the lower part of the stormflow zone and the upper part of the vadose zone than at deeper levels, (3) a larger effective porosity near the top of the vadose zone than at deeper levels, and (4) transpiration losses before the wetting front reaches the water table.

3.4 WATER BUDGET

The geometric mean of seasonal change in water levels of observation wells is 1.5 m (Moore 1988, p. 10). Comparisons of the areas under water level hydrographs indicate that about 80% of the annual recharge and 60% of the discharge occur in the 6-month period from midOctober to midApril. The net increase in water storage during this time causes a water table rise from the seasonal low to the seasonal high. The average annual recharge of the water table can be calculated from these relationships:

$$(0.8Q - 0.6Q) = ns,$$

$$Q = 5ns,$$

where $\underline{n}$ is effective porosity, $\underline{Q}$ is annual groundwater recharge, and $\underline{s}$ is average seasonal rise in the water table. If effective porosity is assumed to be 0.0042, annual recharge is about 3.2 cm of water or 5.7% of streamflow. This rough estimate is nearly the same as that of another calculation discussed later. If 80% of groundwater recharge occurs in a 182-d period from midOctober to midApril and if transpiration losses are ignored, total average recharge in the period is 2.6 cm of water, and

average daily recharge is 0.014 cm of water. Average daily recharge during the other 183 d/yr is only 0.0035 cm of water.

The total range in seasonal fluctuation of the water table is about 0.2-7.6 m. This range is caused by local differences in porosity near the water table, spatial differences in annual recharge, seasonal differences in the relative amounts of recharge and discharge, and seasonal differences in amounts of lateral groundwater flow to and from any location. If the entire range of seasonal water table fluctuations were caused by differences in porosity, the equation above indicates that the range in porosity near the water table would be 8.4×10^{-4} to 0.032. Both end values in this range are reasonable because they represent the upper end of the probable range for fracture porosity in bedrock and the midrange of porosity for saprolite. If porosity is a uniform 0.0042 and if the entire range in seasonal fluctuations of the water table were caused by local differences in annual recharge the resulting range in local recharge would be 0.42-16 cm of water. Both ends of this range are unreasonable, and local differences in porosity may thus be more important than local amounts of annual recharge in determining seasonal fluctuation of the water table. Seasonal differences in the relative amounts of recharge and discharge are probably less important than the other factors because a small seasonal change in water level would mean only a small difference between recharge and discharge rates during both the wet and dry seasons of the year; this situation is unlikely. Local seasonal differences in groundwater inflow and outflow cannot be evaluated.

Most water losses by transpiration occur near the land surface because the numbers of vegetation roots decrease with depth. Nevertheless, tree roots about 1-5 mm in diameter are commonly observed at depths of 2-3 m in saprolite, and smaller roots may reach depths of at least 3-4 m. Also, the capillary fringe is about 1-2 m above the water table in fine-grained soils (Davis and DeWiest 1966, p. 188), and larger capillary rises occur in the smallest pores and along the contacts between grains. Rates of upward water flow are very low for the smallest openings, but a combination of root depth and capillary rise may cause relatively large water losses to depths of 3 m and smaller losses to depths of more than 5 m. In many areas, the seasonal decline of the water table during the growing season is caused partly by transpiration losses and partly by lateral flows toward discharge locations.

The depth of the water table is mostly determined by the local water balance. A shallower or deeper water table would result in a different water loss by transpiration and a different flow rate toward discharge locations. Wells with water depths of less than 1.5 m (Fig. 9) are nearly all in valleys, where relatively large lateral inflows of water come from higher elevations. These belts of shallow water levels commonly extend far up tributary valleys to points near a drainage divide. Water levels deeper than about 9 m (Fig. 9) generally occur in wells at high elevations near the edge of a steep slope, especially a scarp slope; both transpiration losses and groundwater inflows are minimal in these areas. Wells with water levels in the range 1.5-9 m deep occur in areas where there are intermediate amounts of lateral groundwater inflow and transpiration losses and where recharge increases the lateral outflow toward discharge locations.

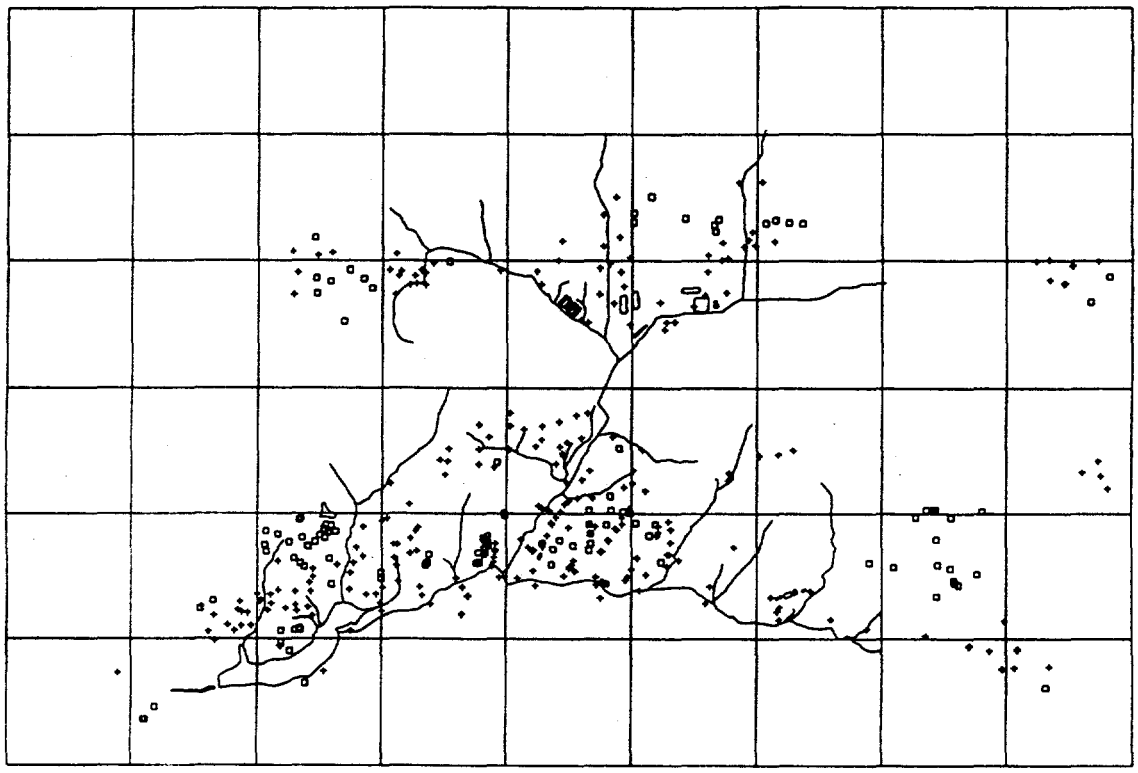

WELLS IN X-10 AREA

+ DEPTH TO WATER < 5 FT.
□ DEPTH TO WATER > 30 FT.

Fig. 9. Observation wells where water levels reach depths of less than 1.5 m (crosses) and more than 9 m (squares).

4. HYDROLOGY OF THE SHALLOW AQUIFER

The shallow aquifer extends from the water table to a depth of about 30 m in the Rome Formation, the Conasauga Group, and the Chickamauga Group. In the Knox Group, the base of the shallow aquifer is at a depth of about 50–100 m. Water-bearing fractures are ubiquitous below the water table, but enlarged fractures and cavities occur only in the shallow aquifer. The larger openings are the targets for wells and constitute the water-producing intervals in wells. The water-producing openings are fed by seepage through matrix fractures, which occur at both shallow and deeper levels. The matrix fractures are more numerous, are connected, and produce the continuity for groundwater flow paths.

Water-producing openings consist of cavities in limy units and of fractures with relatively large apertures in all geologic units. The characteristics of cavities in the study area were described in Moore (1988, pp. 22–32); cavities are not discussed separately in the present report because a single population of hydraulic conductivity values describes both types of water-producing openings.

Differences in the depths of 29 well pairs in the Conasauga Group and the Chickamauga Group show that the geometric mean of the vertical spacing between water-producing intervals is 10.4 m, and the range from the mean minus one to plus one standard deviation is 8.2–12.6 m. Similarly, a probability graph of well depths (Moore 1988, p. 44) shows that within a depth range of 5–25 m, approximately 50% of the wells intercept a water-producing interval in any 5-m interval. This is adequate evidence to

conclude that the average vertical spacing between water-producing intervals is about 10 m. Laterally, the average spatial frequency for water-producing intervals is about 0.92.

4.1 PERMEABILITY AND HYDRAULICS

More than 600 values of hydraulic conductivity have been measured by slug tests (mostly) and other tests in the study area. A cumulative probability graph (Fig. 10) of merged hydraulic conductivity data from both water-producing openings and matrix fractures shows two slopes, thereby indicating two different populations. The upper population represents water-producing intervals in the shallow aquifer, and the geometric mean of hydraulic conductivity is 0.045 m/d. The lower population represents the permeability of matrix fractures; the geometric mean of hydraulic conductivity is 0.00025 m/d. The minimum hydraulic conductivity value in the upper population is the same as the maximum hydraulic conductivity in the lower population and is 0.0052 m/d. However, the break in the slope of the graph shows that both populations are truncated. The complete population of water-producing intervals includes some hydraulic conductivity values smaller than 0.0052 m/d, and the complete population of matrix fractures includes some larger values.

A separate probability graph of hydraulic conductivity data for water-producing intervals (Fig. 11) shows that the geometric mean is 0.041 m/d and that the range from the mean minus one to plus one standard deviation is 0.0065–0.26 m/d. A previous analysis of these data (Moore 1988, pp. 47–55)

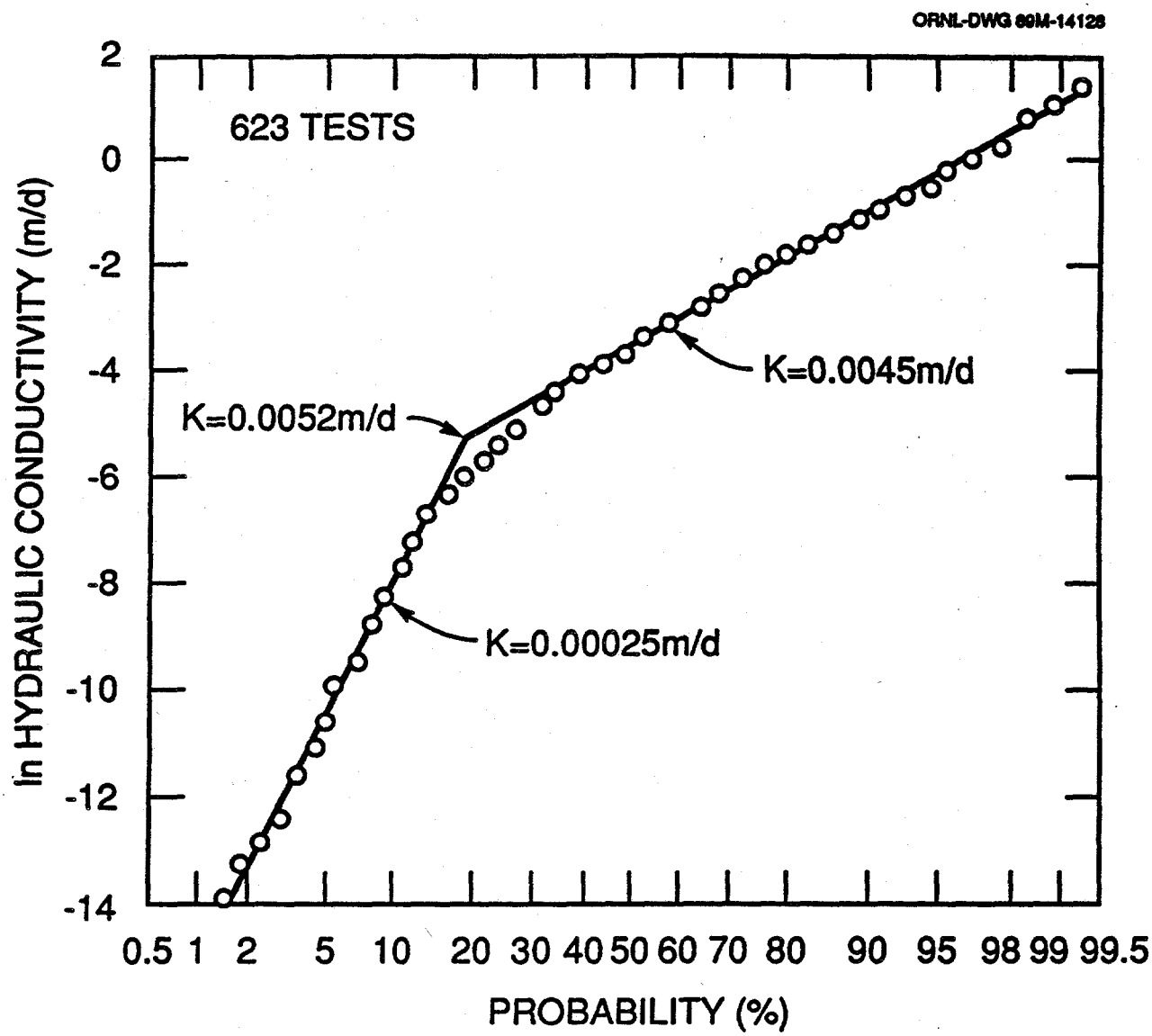

Fig. 10. Cumulative probability graph of merged hydraulic conductivity data for water-producing intervals and matrix fractures.

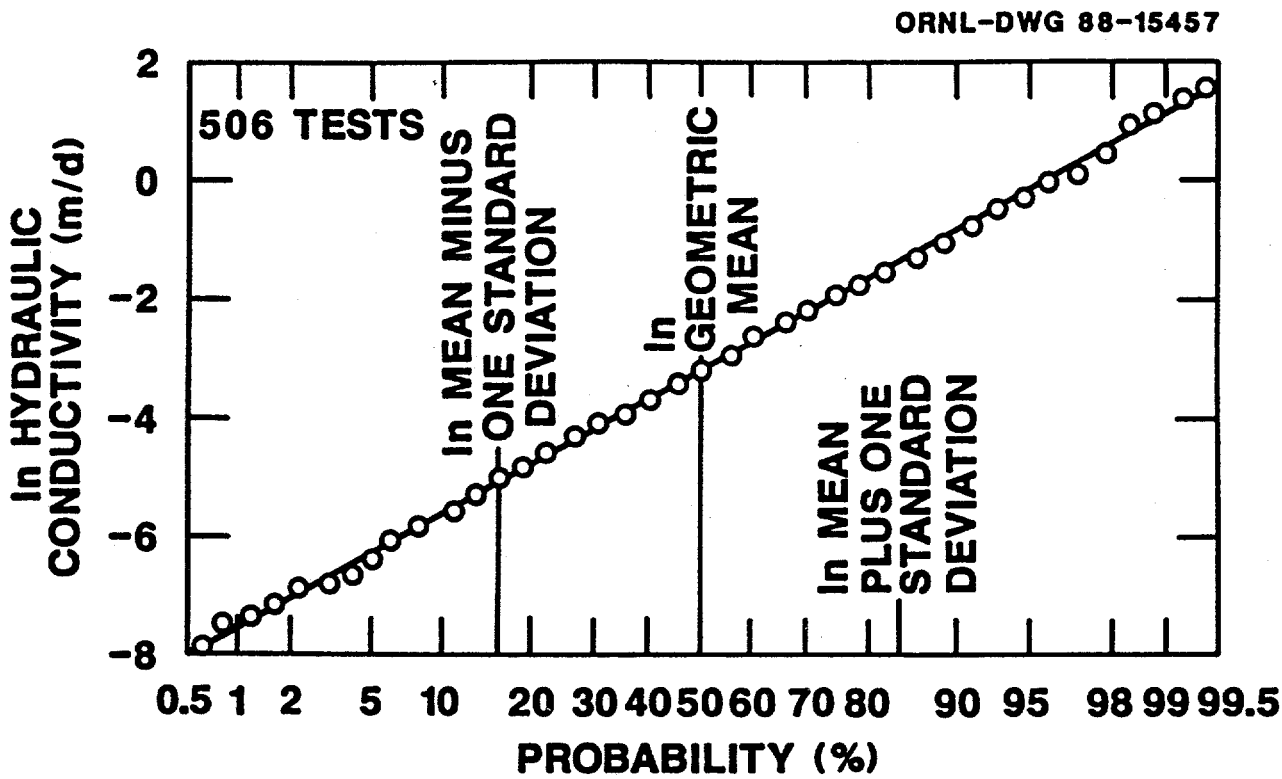

Fig. 11. Cumulative probability graph of hydraulic conductivity data for water-producing intervals.

showed no statistically significant differences in the geometric means of hydraulic conductivity between regolith and bedrock, between depth intervals shallower than 20 m, and between the major geologic units (Rome Formation, Conasauga Group, Knox Group, and Chickamauga Group). However, only a few hydraulic conductivity values are available for the Knox Group, and these data are not representative because most cavities were cased off before the wells were tested. Also, the geometric mean of hydraulic conductivity for dolostone, which occurs mostly in the Knox Group, is statistically larger than that of all other rock types at the 1% level of significance. These observations suggest that if representative data were available, the geometric mean of hydraulic conductivity for the Knox Group would be significantly larger than that of the other geologic units. It was also previously determined that the geometric mean of hydraulic conductivity for wells that were thoroughly developed before testing is about twice as large as that for undeveloped wells. This result shows that the apparent radius of a well is approximately doubled by development. On the other hand, the hydraulic conductivity values for all data classes plot as a single population on the graph. It is also important to note that 13% of the data at the lower end of the graph are within the range that is characteristic of matrix fractures.

The cumulative probability graph of hydraulic conductivity data for matrix fractures (Fig. 12) is somewhat irregular, but a single straight line can be satisfactorily fitted to the data. The geometric mean of hydraulic conductivity is 0.00044 m/d; the difference between this value and that of 0.00025 m/d is caused by the truncation of the population on Fig. 10. On

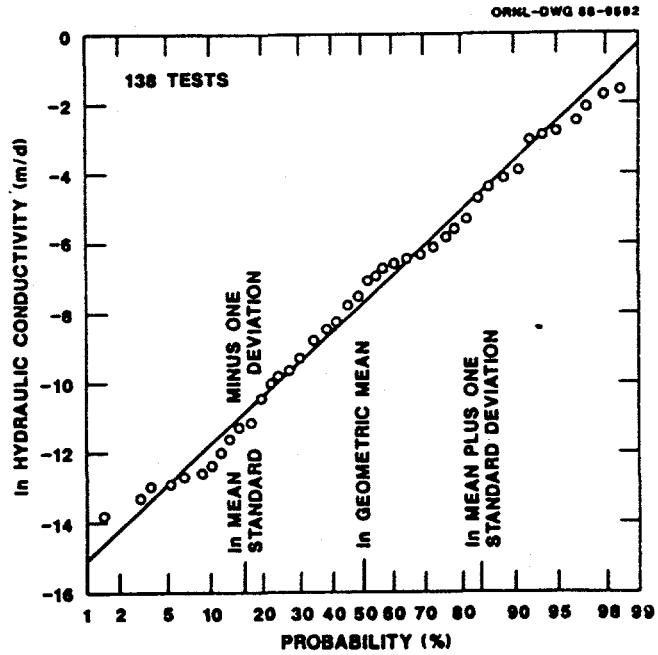

Fig. 12. Cumulative probability graph of hydraulic conductivity values for matrix fractures.

Fig. 12, the range from the mean minus one to plus one standard deviation is 1.8×10^{-5} to 0.011 m/d. About 22% of the values at the upper end of the graph are within the range for water-producing intervals. The overlaps in data ranges on Figs. 11 and 12 suggest that fracture apertures are a continuum in the study area and show that terms such as "matrix fractures" and "water-producing intervals" do not necessarily indicate a large difference in local permeability.

Equations for groundwater flow in a single fracture are based on Darcy's law and the Navier-Stokes equations for laminar flow in a Hele-Shaw (parallel plates) model. As shown in various textbooks (Davis and DeWiest 1966, pp. 241-247, for example) and journal articles, the derivations include the cubic law for linear flow:

$$Q = giwb^3/12v,$$

where $\underline{w}$ is the cross-sectional width of the fracture and $\underline{b}$ is the aperture. The cubic law has been proven experimentally regardless of asperities and loading (Witherspoon et al. 1980, p. 1023). However, contacts at the asperities reduce fluid flow by a factor of $(1/\underline{f})$, which may be related to the decimal percentage of contact area. The experimentally determined range for $\underline{f}$ is 1.00-1.65 (Witherspoon et al. 1980, pp. 1021-1023), which shows that the ideal flow rate is reduced less than 50% by asperity contacts.

Three equations relate aperture to permeability in a Hele-Shaw model:

$$K = gb^2/12v,$$

$$T = gb^3/12v,$$

$$b = T/K,$$

where $\underline{T}$ is transmissivity. These equations show that fracture aperture in

a Hele-Shaw model is theoretically equivalent to the thickness of an unconsolidated aquifer. If wells near ORNL intersect isolated fractures, the T/K ratio values obtained from slug tests would be < 1 mm. The ratio values, instead, have a total range of 0.4-17 m. The average ratio value for any given hydraulic conductivity value (Fig. 13) can be calculated from separate probability graphs for hydraulic conductivity and transmissivity. These average ratio values have a narrow range and increase from about 1.8 m for the least permeable matrix fractures to about 5.0 for the most permeable, water-producing intervals.

The differences between fractured rocks in the study area and Hele-Shaw models are caused by multiple fractures and intersections. In the study area, the matrix fractures are connected with each other and with water-producing intervals. Snow (1969, pp. 1276, 1288) noted that the hydraulic conductivity of an aquifer with multiple fractures is proportional to the average of aperture cubed and inversely proportional to fracture spacing whereas transmissivity is proportional to the sum of aperture cubed.

The general equations for multiple, intersecting fractures are:

$$Q_t = g(iwb^3)_t/12v,$$

$$K = g(wb^3)_t/12vmW,$$

$$T = Km,$$

where $(Iwb^3)_t$ is the sum of the products of aperture cubed, fracture width, and hydraulic gradient; W is the width of the cross-sectional area; and m is the thickness of the water-producing interval (and thus the equivalent of aquifer thickness in porous media).

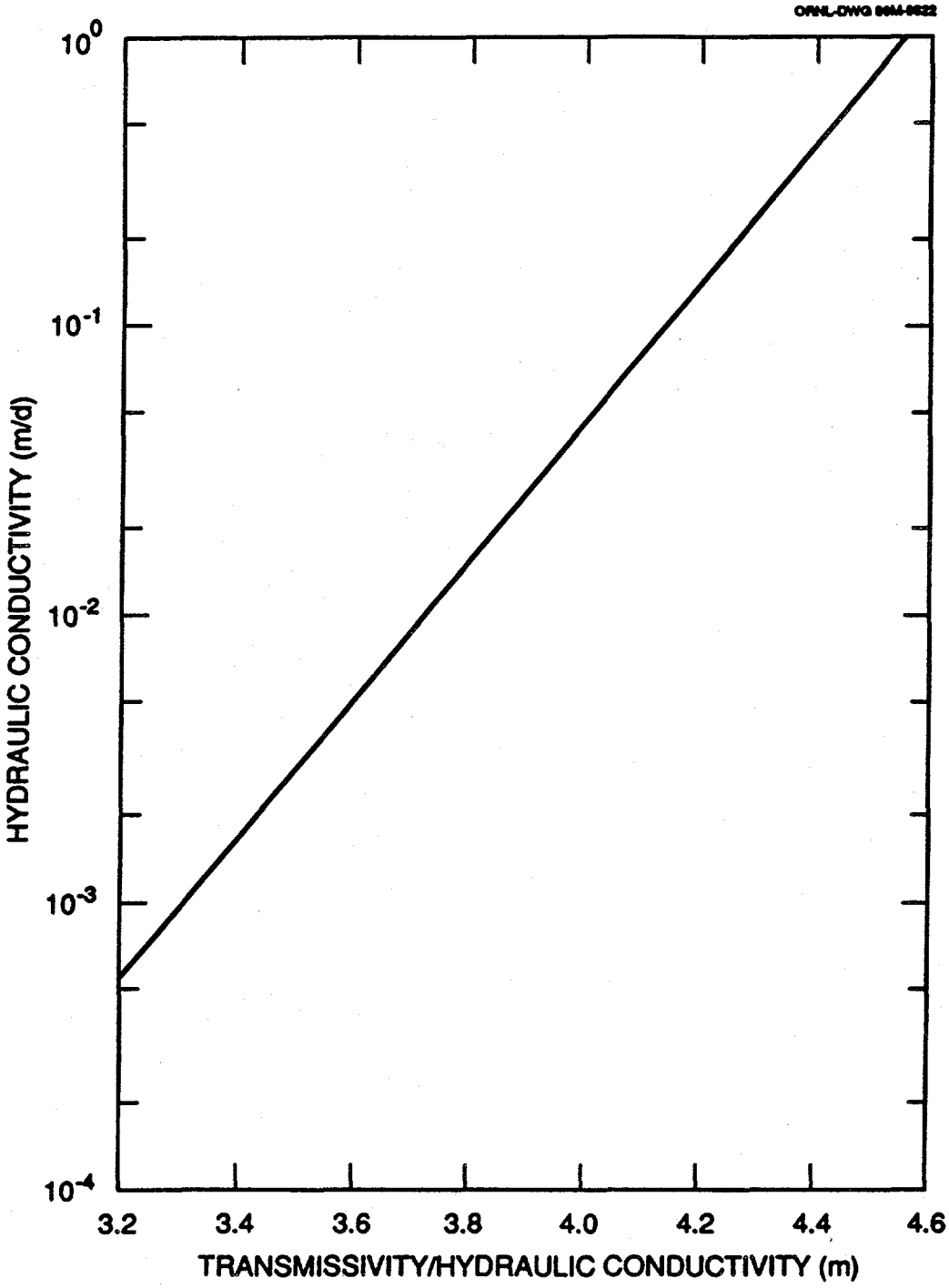

Fig. 13. Relationship between hydraulic conductivity and transmissivity/hydraulic conductivity ratio values.

If some basic hydrogeologic data such as hydraulic conductivity, hydraulic gradient, and porosity are available for a fracture system, other characteristics can be calculated with special forms of the general equations. It is necessary, however, to assume an identical aperture (or a mean aperture cubed) and a mean fracture width and spacing. Hydraulic conductivity is directly proportional to fracture porosity (Snow 1968; Freeze and Cherry 1979, pp. 74-75), and in a unit area,

$$n_f = Nbw/A = Nb, \qquad (4)$$

where n_f is fracture porosity, N is number of fractures, and A is area. The relationships of aperture to hydraulic conductivity are

$$b^2 = 12vK/gn_f, \qquad (5)$$

$$b^3 = 12vK/gN. \qquad (6)$$

Mean fracture aperture can thus be calculated from hydraulic conductivity and an estimate of either fracture porosity or number of fractures in a unit area. The main utility of these equations, however, may be the calculation of fracture porosity from an estimate of fracture density.

4.2 FRACTURE CHARACTERISTICS

Both fracture density and average aperture are probably larger in water-producing intervals than in matrix intervals. Dreier et al. (1987, pp. 54-55) measured a fracture density of 200/m in saprolite of the WAG 6 area, but fewer fractures occur in rock that is less weathered. Sledz and Huff (1981, pp. 44-52) measured a minimum fracture density of 5/m in fresh rock. It may be reasonable to assume that average fracture density is 50-100/m in

water-producing zones and 5-10/m in matrix zones. Because the geometric means of hydraulic conductivity are 0.041 m/d in water-producing zones and 0.00044 m/d in matrix zones, equations (6) and (4), above, can be used to show that the average aperture in water-producing zones is 0.019-0.025 mm, and that fracture porosity is 0.001-0.002. Similarly, the average aperture in matrix zones is 0.009-0.011 mm, and fracture porosity is 6×10^{-5} to 9×10^{-5}. The calculated porosity for water-producing zones is only slightly smaller than the average previously determined by hydrograph analysis (0.0042). In comparison, Smith and Vaughan (1985, pp. 141, 144) measured geometric mean values for storativity of 0.001 and 0.004 for aquifer tests in WAG 6, and the geometric mean of storativity for 24 aquifer tests in Bear Creek Valley is 7.8×10^{-4}. It may or may not be coincidental that all of these results are in the same order of magnitude. The calculations also show, however, that matrix intervals have a much smaller fracture porosity than water-producing intervals.

Most fractures in the Conasauga Group and the Chickamauga Group are short, a few centimeters to 1 m in length, but various joint sets form an intersecting system (Sledz and Huff 1981, p. 12). One of the three common fracture sets is bedding-plane parallel; the other two sets have along-valley (strike parallel) and cross-valley (dip parallel) trends and are steeply dipping (Dreier et al. 1987, p. 53). Other extension or shear fractures may occur in any area and may have local hydrologic significance, but the common fractures form a three-dimensional network of intersecting openings and are adequate to explain groundwater flow in the shallow aquifer.

Within a fracture, groundwater can flow downdip or laterally in either or both of two directions. Changes in flow direction as well as splits and joins of flow paths may occur at fracture intersections, and groundwater flow paths may locally resemble stairsteps in both plan and section views. Tracer tests, however, show that most groundwater flow is nearly parallel to the water table. In a conceptual model of the fracture system (Fig. 14), the trend of water-producing intervals is controlled by bedding planes. Thus, along-valley flow paths are almost entirely within water-producing intervals toward cross-cutting, tributary valleys and streams. Cross-valley flow paths occur partly in water-producing intervals but also cross matrix intervals toward main-valley streams. This model shows that water-producing intervals should be anisotropic and that most groundwater flow should be nearly horizontal.

Previous workers agree that the shallow aquifer is anisotropic and that fracture permeability parallel to geologic strike is larger than in transverse directions. The evidence consists of elliptical drawdown patterns during aquifer tests and differences in arrival times or elliptical concentration patterns observed during tracer tests. The older research on anisotropy was referenced and summarized by Webster (1976, pp. 15-16). Anisotropic drawdown patterns during two recent aquifer tests were shown by Smith and Vaughan (1985). A sensitivity analysis of a digital groundwater flow model was used by Tucci (1985, p. 10) to show that a ratio value of about 3.0 produced the best fit for strike-parallel to strike-normal hydraulic conductivity in Melton valley.

ORNL-DWG 89M-14127

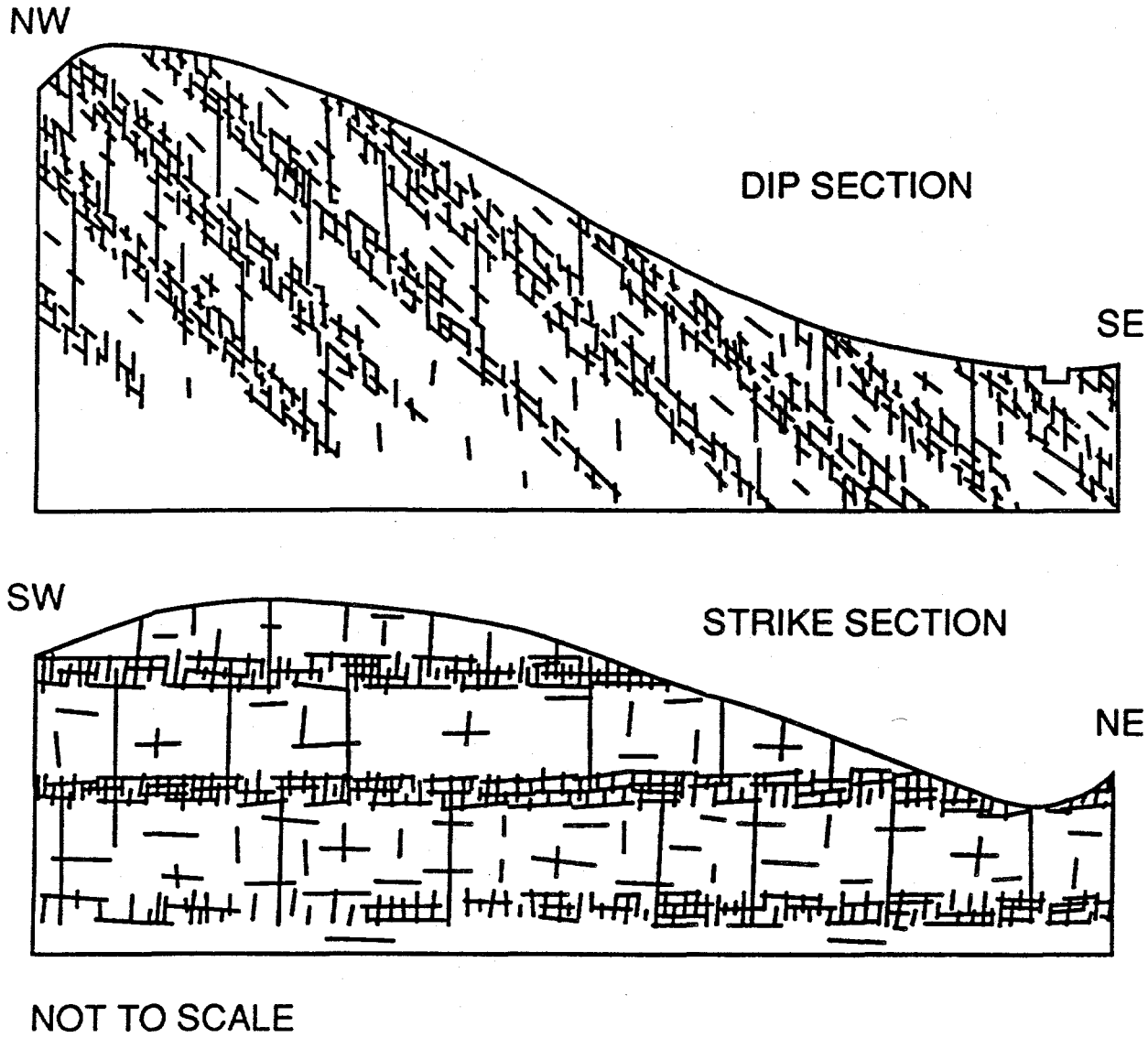

Fig. 14. Sections showing hypothetical differences in trends and densities of fractures near ORNL. A third fracture set in each section is represented by the plane of the paper.

For porous media, advective groundwater flow is in the direction of the maximum hydraulic gradient. In fractured rock, however, groundwater flow occurs in all directions where there are open fractures and a hydraulic gradient. Folds, faults, sealed fractures, and water table rises are common barriers to lateral flow in a fracture system, but in the absence of such barriers, advective flow from one point in one fracture may eventually occupy a semicylindrical volume of the aquifer. Splits and joins of the flow paths have considerable importance for the spread of pollutants from a source near the water table, and various amounts of longitudinal dispersivity may occur along all branches of the flow paths.

Calculations of hydraulic gradient assume linear flow paths between the points where potentiometric heads are measured. In fractured rocks, path length between two points may be nearly the same as map distance in the directions of the fracture sets. In other directions, the length of a stairstep path is up to 1.4 times longer than map distance (the sum of equal X and Y distances, 2a, divided by diagonal distance, $2^{0.5}a$) in a two-dimensional view and up to 1.7 times longer in three dimensions. Path length corrections are generally unnecessary for calculations of hydraulic gradient because map distance errors are small and because both permeability and porosity are spatially variable.

Measurements near the WAGs indicate a range of 0.01-0.1 for cross-valley hydraulic gradient; the average gradient near the water table is about 0.05. In the along-valley direction, the hydraulic gradient has a range of 0.001-0.01 and the average may be about 0.005. A hydraulic gradient in the range for cross-valley flow may also occur along strike on

the slopes of tributary valleys. Gradients near the lower ends of these ranges occur in relatively flat areas and gradients closer to the upper ends occur on steeper slopes. However, any apparent hydraulic gradient larger than about 0.06 may represent a cascade, a different flow path, or other discontinuity in flow and should be considered suspect. Smaller hydraulic gradients would be expected at deeper levels in the aquifer, but at depths of about 20 m, gradients are not greatly different than those near the water table in the Conasauga Group and the Chickamauga Group. Smaller hydraulic gradients are shown at depths of 30–70 m on sections of Melton Valley by Webster and Bradley (1987, pp. 82, 89) but are based on sparse data.

4.3 FLOW RATE

The best approach to calculation of average groundwater flow rate in the shallow aquifer is uncertain because of (1) truncated populations of hydraulic conductivity values for water-producing intervals and matrix fractures, and (2) large flow rates in a small percentage of fractures with large apertures. One method consists of integrating the areas under the probability curves for hydraulic conductivity in order to obtain the mean flow rate for each population. Assume first that cross-valley flows of groundwater are mostly in matrix fractures and that the controlling hydraulic gradient is 0.05. For flow through a tube 1 m wide and 30 m high (eq. 3), the calculated average hydraulic conductivities, average transmissivities, and flow rates are shown in the data below.

Probability (%)	K (m/d)	T (m^2/d)	Q (m^3/yr)
0-10	3.5×10^{-6}	1.1×10^{-4}	1.9×10^{-4}
10-20	2.0×10^{-5}	6.1×10^{-4}	0.0011
20-30	6.1×10^{-5}	0.0018	0.0034
30-40	1.4×10^{-4}	0.0043	0.0078
40-50	3.0×10^{-4}	0.0091	0.017
50-60	6.6×10^{-4}	0.020	0.036
60-70	0.0015	0.044	0.080
70-80	0.0034	0.10	0.18
80-90	0.010	0.30	0.55
90-100	0.17	5.2	9.5
TOTAL			10.3
MEAN	0.019	0.57	

The most permeable 10% of the matrix fractures transmit 92% of the groundwater flow, and the hydraulic conductivity for the mean flow rate is 0.019 m/d, which is near the geometric mean of hydraulic conductivity for water-producing intervals.

Second, assume that some groundwater flow will occur along strike toward tributary valleys and other topographic depressions, that this flow occurs mainly in three water-producing intervals aggregating 12 m thick, and that the hydraulic gradient is 0.005. For flow through a tube 1 m wide and 12 m high (eq. 3):

Probability (%)	K (m/d)	T (m^2/d)	Q (m^3/yr)
0-10	0.0019	0.023	0.0042
10-20	0.0058	0.070	0.013
20-30	0.012	0.14	0.026
30-40	0.020	0.24	0.044
40-50	0.032	0.38	0.070
50-60	0.051	0.61	0.11
60-70	0.082	0.98	0.18
70-80	0.14	1.7	0.31
80-90	0.29	3.5	0.64
90-100	1.5	18	3.3
TOTAL			4.7
MEAN	0.21	2.6	

The most permeable 10% of the fractures transmit about 70% of the flow in water producing intervals, and the average hydraulic conductivity for the total flow is about the same as the geometric mean plus one standard deviation for the population.

Total groundwater flow from a tube 1 m wide is larger than the 10.3 m^3/yr calculated for cross-valley flow but smaller than the 15.0 m^3/yr calculated as the sum of cross-valley and along-valley flows. The average annual flow in a large number of tubes may be about 12.5 m^3. In comparison, Moore (1988, pp. 68-69) used separate geometric means of 0.041 and 0.00044 m/d for hydraulic conductivity in water-producing intervals and matrix fractures and assumed a constant hydraulic gradient of 0.05 to calculate a combined flow rate of 9.1 m^3/yr in a flow tube 1 m wide and 30 m high. Both sets of assumptions and results are reasonable. Other combinations of parameter values can be used to calculate larger flow rates. However,larger flow rates are not supported by records of water level fluctuation and calculations of effective porosity and recharge amounts, as discussed previously. The exact combination of parameter values that determine groundwater flow rates toward discharge locations is unknown, but trial calculations and a convergence of other evidence indicate that a flow rate of 12.5 m^3/yr is approximately correct for a tube 1 m wide and 30 m high.

4.4 PATH LENGTH

A consideration of average and maximum distances to streams in the study area indicates that the lengths of groundwater flow paths do not

exceed about 400 m and may average about 200 m (Moore 1988, pp. 63, 67). Approximately this same result is obtained by calculations. If the shallow aquifer extends to a depth of 30 m and if the average slope of the land surface is 0.075, the maximum horizontal path length (30/0.075) is 400 m. Previously in this report, a path length of 455 m was calculated as the average maximum distance to a flowing stream at the time of a 50% duration streamflow. If recharge occurs evenly on a flow tube 1 m wide and 400 m long, and if discharge from the tube is 12.5 m^3/yr, the average recharge rate is 3.1 cm/yr of water, or 5.5% of streamflow. In comparison, a recharge rate of 3.2 cm/yr of water was calculated previously from estimates of effective porosity and the times when recharge occurs.

4.5 WATER DISCHARGE

As discussed previously, the depth to the water table at any location and time is determined by the local water balance and represents the results of recharge, lateral groundwater inflow, lateral groundwater outflow, and discharge processes. The net effect of these processes is similar in nearby areas, and it has been commonly noted that "the water table is a subdued replica of land surface" (Stockdale 1951, pp. 50-51). One of the processes in a local water balance is flow through the shallow aquifer toward the streams. Some water undoubtedly flows laterally and upward from the shallow aquifer through the stormflow zone and discharges into the streams. The shallow aquifer has an average hydraulic conductivity of 0.041 m/d and is capable of transmitting about 170 m^3/yr of water toward the streams in each

1 km^2 of drainage area; if all of this water were discharged to the streams, it would be equivalent to the 84% duration streamflow. The lateral hydraulic gradient in valley areas is about 0.015. Based on these data and eq. (3), all of the water in the shallow aquifer could be transmitted into the stormflow zone in a strip 56 m wide on each side of a stream. This size of area is reasonable, but as discussed below, there is good reason to believe that only a part of the water in the shallow aquifer reaches the streams.

Flow paths ending at the streams are inadequate to explain (1) the close correspondence nearly everywhere between the configurations of the land surface and the water table, (2) the close correspondence in most areas between the water table and top of bedrock, and (3) the large decreases in apparent hydraulic gradient at the bases of the ridges. These features would not occur if water is added to the aquifer by recharge along the flow paths. A water table is a free surface, the slope and shape of which are determined by relative rates of recharge and discharge. In the study area, there is no inherent hydrologic link between the configuration of the land surface and that of a water table at depth. Also, a decrease in hydraulic gradient along a flow path must correspond with water discharge or with an increase in hydraulic conductivity. Significant changes in average hydraulic conductivity do not occur at the bases of steep slopes or at other landform locations. These facts suggest a different hydrologic process, one in which water is discharged from the shallow aquifer along the flow paths and a process in which the relative elevations of the land surface and the water table control discharge rates. In turn, the locations and rates of

this water loss determine the position of the water table. Lateral flows above the water table may occur under saturated, tension-saturated, or partly saturated conditions. As noted previously, groundwater may be discharged by transpiration wherever the water table is less than 2-3 m below the surface.

Water-producing openings have a geometric mean of hydraulic conductivity about 100 times larger than that of matrix fractures, and enlarged fractures and cavities are known to occur above the water table. This large contrast in permeability may be important in the lateral transmission of groundwater, above the water table, from the shallow aquifer toward the stormflow zone. The average length and hydraulic gradient for flow paths leading from the water table to the stormflow zone can be determined by calculation. The stormflow zone has an average thickness of about 1.2 m. The geometric mean of depth to the water table in October is 4.1 m, but the population includes large values at locations where local discharge processes may be relatively unimportant. Thus, the water table may have an average depth of 2-3 m below the base of the stormflow zone. If the average slope of the stormflow zone is 0.075, the average discharge path length (2.0/0.075 or 3.0/0.075) is 27-40 m. Most well hydrographs (Fig. 8) show small rates of water-level decline during dry seasons of the year. This fact suggests that the hydraulic gradients for discharge along lateral flow paths are determined by seasonal fluctuations of the water table, even though the amount of fluctuation is commonly a small percentage of the height of the water table above the closest stream. Because the geometric

mean of seasonal change in the water table is 1.5 m, the hydraulic gradient along an average lateral flow path (1.5/27 or 1.5/40) at the time of the seasonal high water table is 0.038–0.056. A gradient in this range is nearly the same as the average slope of the water table and thus may explain the nearby discharge of some of the water received as recharge in an average year.

In further development of the concept, the water table occurs at a depth where there is a water balance. Changes in elevation of the water table produce only small changes in hydraulic gradient along flow paths leading to the streams, and groundwater flow rates along these paths are nearly constant. Conversely, water table rises apparently cause a proportional increase in the rate of lateral flow toward the stormflow zone, and water table declines decrease these flows. It probably is significant that a falling water table during a severe drought would be retarded by drainage from the regolith, which requires a period of up to 45 d. It may also be significant that capillary rises in fractures apertures of >0.015 mm are less than 1 m, and effective porosity is small in the bedrock; little tension-saturated flow would occur below the top of bedrock. These properties suggest that lateral flows above the water table are near zero when the water table is below the top of the bedrock but increase progressively when the water table rises in the regolith. A process of this type is needed to explain the close correspondance of the water table and the top of bedrock. If this hypothesis is correct, the shallow aquifer is capable of more water discharge than is received as recharge because the

average depth of the water table is 2-3 m below the stormflow zone. Local hydrologic flow patterns and processes may be recharge limited.

The lateral flow and discharge of groundwater above the water table would explain the similar configurations of the land surface and the water table. The resulting decrease of groundwater flow rates in the shallow aquifer would also explain abrupt decreases in hydraulic gradient near the bases of slopes. Third, increases and decreases in this flow through time would limit the amounts of water table fluctuation during wet and dry periods. Fourth, the near-surface flow of groundwater from the shallow aquifer would support the continued healthy growth of trees on steep hillsides during droughts. Fifth, a decreased lateral flow above the water table when water levels are relatively low, but still far above the level of the streams, could explain the nearly flat bases of observation-well hydrographs. Finally, the lateral flow of groundwater toward the stormflow zone could explain hea bedrock water chemistry in many shallow wells; a similar water chemistry should occur in the stormflow zone at relatively low elevations.

If saturated flow were to begin in enlarged fractures above the water table, leakage into the tension-saturated or partly saturated matrix would occur along the lateral flow path. Assuming that the hydraulic conductivity of the matrix is 0.00044 m/d (the geometric mean for saturated conditions) and that the hydraulic gradient is 1.0, seepage from a tube 1 m wide along a flow path that is 27-40 m long would be 4.3-6.4 m^3/yr. The seepage losses from a single enlarged fracture thus would be 35-50% of total groundwater flow in a tube that is 30 m high. Nearly all flows above the water table

therefore probably occur under tension-saturated or partly saturated conditions. For partly saturated conditions within the matrix, water should drain vertically until it returns to the water table or until it reaches another large fracture. Flows in the vadose zone may thus resemble stairsteps, where flow is lateral under tension-saturated conditions and vertical under partly saturated conditions. Groundwater discharge may occur partly or mostly as transpiration losses because flow paths lead toward shallower depths.

The lateral flow of groundwater along fractures above the water table is speculative but is reasonable and explains the available data. One remaining uncertainty in determining the local water balance is the relative importance of lateral flow above the water table in comparison with saturated flow below the water table and transpiration loss at any level. Another uncertainty is whether tension-saturated flows, especially any chemical constituents and contaminants in the water, eventually reach the stormflow zone and the streams. Solutions to these problems will require new data although information might also be obtained with a digital model of unsaturated-saturated flows.

5. HYDROLOGY OF THE DEEPER AQUIFER

The deeper aquifer occurs below any water-producing intervals and generally has the same characteristics as matrix intervals within the shallow aquifer. The fracture porosity of the deeper aquifer has not been determined but probably is smaller than water-producing intervals of the shallow aquifer. There is a smaller spatial frequency of open fractures at depth, and average aperture is smaller because of a larger overburden pressure. A typical effective porosity in the deeper aquifer might be in the range 1×10^{-5} to 1×10^{-4}. The geometric mean of hydraulic conductivity in the deeper aquifer is 0.00044 m/d, and the range from the mean minus one to plus one standard deviation is 1.8×10^{-5} to 0.11 m/d (Fig. 12).

All water in the deeper aquifer occurs under confined conditions. This water comes from shallower levels and eventually returns to shallow levels before discharge to streams and by evapotranspiration. However, the small geometric mean of hydraulic conductivity in the deeper aquifer, as compared to water-producing intervals in the shallow aquifer, indicates that rates and quantities of groundwater flow are much smaller than in the shallow aquifer. Groundwater flows in the shallow aquifer can be called slow seepage in comparison to flow rates in the stormflow zone. Similarly, flows in the deeper aquifer can be called slow seepage in comparison to those in the shallow aquifer.

Groundwater flow paths in the deeper aquifer have longer vertical segments than those in the shallow aquifer, and the hydraulic gradients for

lateral flow are therefore smaller. Along a flow path that extends to a depth of 65 m, for example, average path length would be about 300 m, instead of 200 m in the shallow aquifer; the average hydraulic gradient for this deeper path would be about 0.033 compared with 0.050 in the shallow aquifer. If the deeper aquifer is assumed to average 100 m thick, if hydraulic conductivity is 0.00044 m/d, and if average hydraulic gradient is 0.035, the groundwater flow rate through a tube 1 m wide (eq. 3) is 0.56 m^3/yr. This flow rate is only 4.5% as large as that in the shallow aquifer.

There is periodic speculation about the possibilities of deep groundwater flow, especially along faults, and thus of contaminant transport beneath drainage divides to off-site wells and springs. In considering these possibilities, it is significant that off-site groundwater flows have not been detected in the ORNL area during 40 yr of study. If such flows occur, they must be localized and uncommon. Groundwater flows unrelated to surface topography generally require intergranular permeability and continuously confined conditions from recharge area to discharge area. In rocks where the only significant permeability is fractures, even local interbasin flows of groundwater are rare, apparently because of numerous discontinuities along the fracture flow paths.

Elsewhere in the fractured rock aquifers of Tennessee, interbasin movement of groundwater has been observed (1) in the Knox Group of Middle Tennessee (Newcome and Smith 1962), (2) along a few faults such as at Cades Cove, Great Smoky Mountains National Park (W. M. McMaster, USGS, personal

communication, 1970), and (3) rarely along fractures or cavities from one valley with a relatively high surface elevation to an adjacent deeper valley (Moore and Wilson 1972, pp. 25–27). Groundwater flow in the Knox Group of central Tennessee is mainly through interconnected pores and vugs (Newcome and Smith 1962, pp. 14, 16), which have not been reported in the ORNL area.

In the Conasauga Group and the Chickamauga Group, along-valley groundwater flow across low surface-water divides and into an adjacent drainage basin should be considered as a possibility in limestone formations and members. Because of interbedded shales, a low average permeability, and the resulting likelihood of discontinuities along fracture flow paths, however, groundwater flow beneath the main ridges and beneath the Clinch River is hydrologically nearly impossible. In the Knox Group, conversely, hand, openings with a relatively large aperture are common at deeper levels, and large rates of groundwater flow probably occur at these levels. Cross-strike flows of groundwater beyond the valleys that bound the outcrop belt of the Knox Group are virtually impossible, but along-strike flows within the outcrop belt may occur for distances of at least a few km. For the Knox Group, additional data are needed to fully evaluate the possibility of along-strike flows of groundwater across discharge areas like the Clinch River.

6 APPROACH TO MODELING

The groundwater hydrology of the ORNL area is complex, as has been shown by discussions of the separate characteristics and zones. The problems for digital modeling include transient flows and saturated-unsaturated flow boundaries that have changing locations, changing parameter values, and changing conditions through time. It is clear that steady-state models of saturated flow in porous media have limited utility where a majority of all groundwater flow is transient and occurs in the root zone of vegetation (stormflow zone). Remedial actions and engineering decisions should be based on models that simulate actual flow processes or include surrogates for these processes.

It should be possible to develop a better understanding of the interrelationships between flow parameters and boundary conditions by analyzing the results of one-dimensional or two-dimensional finite-element models (in section format) of saturated-unsaturated flows. If so, water budget and contaminant transport models of relatively uniform areas near the solid waste management units should also prove practical. Finite-element models of saturated-unsaturated flows have been developed for the ORNL area (Reeves and Duguid 1975; Yeh and Ward 1980; Yeh 1987; Yeh 1988), but have been little applied for this purpose. The reasons include the difficulties of modeling transient flows and uncertainty about the values of parameters needed to begin the modeling process. The present report develops estimates of the necessary parameter values.

Saturated-unsaturated modeling of subsurface water flow is not a trivial task. As described by Reeves and Duguid (1975, pp. 5-6), the input data include (1) surface elevations, (2) regolith thickness, (3) soil horizon depths and properties, (4) hydraulic conductivities and storativities of saturated materials, (5) a curve of hydraulic conductivity versus pressure and a curve of water content versus pressure for unsaturated materials, (6) locations and types of initial boundary conditions, (7) times and periods of precipitation and drainage, and (8) water depths in streams and ponds. The boundary conditions (Yeh 1988, pp. 2-4) may include Dirichlet (specified pressure), Neumann (specified gradient), Cauchy (specified flux), and variable types (Cauchy or Dirichlet, depending on conditions); boundary types may also be time dependent with either gradual or abrupt changes in conditions. All interim and final model results must be fully evaluated, and the verification process may include the need for new field data. Kirkby (1988, p. 331) describes modeling efforts of this type as requiring "a very considerable investment in instrumentation and computer time." The final product, however, should be a realistic and reasonably accurate simulation of flow and chemical transport processes in the area of interest.

7. FUTURE RESEARCH NEEDS

The most important objective of the groundwater research program at ORNL is the development of information for the design and support of remedial actions. One problem at present is very few data on the thickness, permeability, and chemical characteristics of water in the stormflow zone, even though a large majority of all groundwater flow occurs in this zone. Infiltrometer tests for measurements of hydraulic conductivity are needed in both natural and disturbed soils of various types at different depths and across the range of land cover types and conditions. Next, the times and depths of saturated flow in the stormflow zone at different topographic locations during different rainfall events need to be measured and monitored; data of this type will be needed for calibration and validation of saturated-unsaturated flow models. Finally, the chemical characteristics of water in the stormflow zone need to be determined. An acidic water with low specific conductance would be expected from upslope locations, but an alkaline, calcium bicarbonate water type would be expected from downslope locations.

A second problem area for research is the use of appropriate digital models for more accurate calculations of parameter values and flow processes. Finite-element models of saturated-unsaturated flow have been developed at ORNL and are likely to produce satisfactory results. Models that simulate only steady-state flows below the water table are less appropriate for the complex hydrologic processes in the ORNL area.

A third research area is determination of the importance of water interchange between the stormflow zone and the shallow aquifer. These processes affect contaminant transport and the downslope discharge of groundwater and contaminants. Monitoring of water contents, pressure heads, and chemical quality of water in the vadose zone will probably be necessary for model validation. Similarly, the relative importance of transpiration losses from the water table versus lateral saturated-unsaturated flows toward the stormflow zone needs to be determined. Only a small percentage of all groundwater flow is below the water table, but the shallow aquifer is a reservoir for contaminants in some areas.

A fourth research problem is that the three-dimensional fracture system in the shallow aquifer is only partly understood. Special arrays of closely spaced wells and three-dimensional tracer tests will probably be required to obtain a detailed picture of fracture connections and discontinuities, anisotropy, hydraulic gradients, and groundwater movement along multiple, alternative flow paths. Also, more accurate values of both aquifer storativity and fracture porosity will soon be required for the modeling of contaminant transport and for design of dewatering facilities. At present, estimates for the average porosity of the shallow aquifer range from about 1×10^{-5} to more than 0.01. Within an aquifer 1 km^2 and 30 m thick, these porosity estimates indicate a storage capacity ranging from 300 m^3 to more than 300,000 m^3 of water. Prolonged pumping tests or aquifer tests are essential for obtaining the required data.

The unknown factors, processes, and configurations are not critical constraints on remedial investigations and actions in the WAGs. The

conceptual model of groundwater occurrence and flow in this report and in Moore (1988) can be used for preliminary planning. However, the additional research is needed to ensure that (1) contaminant sources are hydrologically isolated, (2) contaminants do not overflow or otherwise bypass the monitoring network, and (3) groundwater flow paths are adequately understood in contaminated areas and in future burial grounds. Also, the additional information is needed for model calibration and validation. A modest level of well-planned groundwater research over the next 5 yr should conservatively save 10-20 times its cost by minimizing construction in remedial action programs.

8. CONCLUSIONS

The land surface is permeable in the ORNL area, and nearly all precipitation infiltrates. The majority of this water (an annual average of 76 cm) replenishes soil water and is later consumed by evapotranspiration. Most of the remaining water (an annual average of 56 cm) moves through the ground to discharge locations and produces the natural streamflow.

Groundwater occurs in a stormflow zone that extends from land surface to a depth of 0.3-2 m and in shallow and deeper aquifers that extend from the water table to the base of fresh water. The stormflow zone may be formed by the roots of vegetation. It is thicker and more permeable in forested areas than in grassy and brushy areas; it is also more permeable at the land surface than at deeper levels. A thin vadose zone generally separates the stormflow zone and the shallow aquifer, but the water table is in the stormflow zone near the streams. The openings for groundwater flow below the water table are fractures and cavities. Fractures are ubiquitous, but enlarged openings constitute the water-producing intervals in wells. The water-producing openings occur only in the shallow aquifer, above depths of 20-30 m in the Conasauga Group and the Chickamauga Group. The geometric mean of hydraulic conductivity for water-producing intervals is about 100 times larger than that of the deeper aquifer and of other intervals in the shallow aquifer.

Groundwater is unconfined in the stormflow zone and near the water table, but there is a gradual change to confined conditions at deeper levels. In the Conasauga and Chickamauga groups, the geometric mean depth

to the water table in October is 4.1 m, and the geometric mean depth of the first water-producing interval is 8.2 m. The average thickness of a water-producing interval is 4.0 m, and the average vertical spacing between these intervals is 10 m. Flow paths in the shallow aquifer may be nearly linear or complex. Along a single fracture, groundwater may flow downdip or laterally in either or both of two directions. Changes in flow direction may occur at fracture intersections as may splits and joins of the flow paths. Multiple flow paths connect most points in the aquifer, but discontinuities are also common in some areas.

During precipitation events, the initial increase in streamflow results from rain falling on stream channels and adjacent wetlands. Soon afterwards, streamflows increase because of contributions from storm-drain systems, impervious areas, and more distant wetlands. For larger amounts or prolonged periods of precipitation, however, a large percentage of streamflow represents groundwater discharge from the stormflow zone. During droughts, drainage of water in the stormflow and vadose zones continues, and the discharge of this water constitutes most of the decreasing base flows of the streams.

Water storage in the stormflow zone is intergranular, but the openings for lateral flow are macropores and mesopores. The decimal volume fraction that is available for water storage in the stormflow zone is about 0.15, and the volumetric porosity for flow through macropores and mesopores is about 0.002. The geometric mean of hydraulic conductivity in forested areas decreases from 8.8 m/d at a depth of 15 cm to about 0.011 m/d at a depth of 120 cm. Infiltration first replenishes any soil water deficit in the root

zone; continued infiltration causes a perched water table at the level where percolation rate exceeds hydraulic conductivity. In saturated material below a perched water table, water flows laterally toward wet-weather springs and streams. Water outflow from the stormflow zone occurs by evapotranspiration, percolation down to the water table, and discharge to streams. About 80% of the 10% duration streamflow is groundwater discharge, nearly all of which comes from the stormflow zone. The discharge rate at this time is about 0.26 cm/d of water. The calculated drainage density is 4.6 km^{-1}, and the average subsurface path length is 110 m.

A vadose zone occurs between the stormflow zone and the shallow aquifer in most of the study area. Water is added to the vadose zone by vertical percolation from the stormflow zone and by lateral flow from the shallow aquifer. Water leaves the vadose zone as transpiration and as recharge to the shallow aquifer. The geometric mean of hydraulic conductivity in the vadose zone is 0.0019 m/d. Hydrographs of observation wells show that recharge causes a water table peak in <1-4 d in some areas. In other areas, separate periods of infiltration merge to produce a single recharge event that lasts for a longer period. Daily rises of the water table in response to recharge have a range of 1-200 cm, and the time delay for a water table peak after a precipitation event is 1-45 d. The average linear velocity of water in the vadose zone is 0.02-50 m/d. Calculations based on these data show that the effective porosity near the water table has a range of 8.4×10^{-4} to 0.032. Annual recharge to the shallow aquifer is about 3.2 cm of water or 5.7% of streamflow.

The depth to the water table at any location and time is determined by the local water balance and represents the results of recharge, lateral groundwater flows, and discharge. However, groundwater flows below the water table cannot explain (1) the close correspondence of the water table and top of bedrock, (2) the similar configurations of the land surface and the water table, and (3) large decreases in the hydraulic gradient near the bases of the ridges. Water-producing openings in the shallow aquifer have a geometric mean of hydraulic conductivity about 100 times larger than that of the matrix fractures, and groundwater apparently is transmitted laterally, above the water table, toward the stormflow zone along these enlarged fractures. Most of this flow may occur at less than atmospheric pressure, but the average hydraulic gradient along a lateral flow path connecting the water table to the stormflow zone (0.05) is about the same as for lateral flow below the water table. These relationships show that some of the water received as recharge at the water table is discharged by transpiration. Thus, the water table is not a boundary for lateral groundwater flow but results from the flow processes; the water table has a location and depth determined by lateral distance to the stormflow zone (and the land surface). The remainder of the recharge follows flow paths below the water table to discharge locations in the streams.

The shallow aquifer extends from the water table to a depth of about 30 m in the Rome Formation, the Conasauga Group, and the Chickamauga Group. Enlarged fractures and cavities comprise water-producing intervals in the aquifer and have an average thickness of 4 m and a vertical spacing of 10 m.

The geometric mean of hydraulic conductivity is 0.041 m/d in the water-producing intervals and 0.00044 m/d in matrix intervals. Calculations show a fracture porosity of about 1.5×10^{-3} for water-producing intervals and 7.5×10^{-5} for matrix fractures. The average hydraulic gradient near the water table is about 0.0005–0.05, and groundwater flow through a tube 1 m wide and 30 m high is about 12.5 m^3/yr. If average path length is 200 m, then the shallow aquifer discharges an average 170 m^3/d in each 1 km^2 of drainage area.

The deeper aquifer occurs below any water-producing openings and has the same characteristics as matrix intervals in the shallow aquifer. The water comes from shallower levels and eventually returns to the shallow aquifer and the stormflow zone before discharge to streams and by evapotranspiration. Flow paths are somewhat longer, and the average hydraulic gradient is smaller than in the shallow aquifer. The flow rate through a tube 1 m wide and 100 m high is about 0.56 m^3/yr, which is about 4.5% as large as that in the overlying shallow aquifer.

Steady-state digital models of saturated flow have limited utility for the flow processes in the ORNL area because groundwater flow in the stormflow zone is transient in most areas and because some to most discharge from the shallow aquifer occurs above the water table. Instead, finite-element models of saturated-unsaturated flow can be used to simulate the subsurface flow processes, to provide insight into the interrelationships between parameter values and boundary conditions, and to evaluate water budget and contaminant transport processes. Appropriate models have been developed at ORNL and are available for these purposes.

REFERENCES

Bouwer, Herman. 1978. Groundwater Hydrology. McGraw-Hill, New York.

Davis, E. C., W. J. Boegly, Jr., E. R. Rothschild, B. P. Spalding, N. D. Vaughan, C. S. Haase, D. D. Huff, S. Y. Lee, E. C. Walls, J. D. Newbold, and E. D. Smith. 1984. Site characterization techniques used at a low-level waste shallow land burial field demonstration facility. ORNL/TM-9146.

Davis, S. N., and R. J. M. DeWiest. 1966. Hydrogeology. John Wiley, New York.

Dreier, R. B., D. K. Solomon, and C. M. Beaudoin. 1987. Fracture characterization in the unsaturated zone of a shallow land burial facility. pp. 51-59. IN Flow and Transport Through Fractured Rock. American Geophysical Union Monograph 42.

Freeze, R. A., and J. A. Cherry. 1979. Groundwater. Prentice-Hall, Englewood Cliffs, New Jersey.

Hewlett, J. D., and W. L. Nutter. 1970. The varying source area of streamflow from upland basins. pp. 65-83. IN Interdisciplinary Aspects of Watershed Management. American Soc. Civil Eng., Proceedings. Bozeman, Montana.

Ketelle, R. H., and D. D. Huff. 1984. Site characterization of the West Chestnut Ridge site. ORNL/TM-9229.

Kirkby, Mike. 1988. Hillslope runoff processes and models. Jour. of Hydrology 100:315-339.

Luxmoore, R. J., B. P. Spalding, and I. M. Munro. 1981. Areal variation and chemical modification of weathered shale infiltration characteristics. Soil Sci. Soc. Am. J. 45(4):687-691.

McMaster, W. M. 1967. Hydrologic data for the Oak Ridge area, Tennessee. U.S. Geol. Surv. Water-Supply Pap. 1839-N.

Moore, G. K. 1988. Concepts of groundwater occurrence and flow near Oak Ridge National Laboratory, Tennessee. ORNL/TM-10969.

Moore, G. K., and J. M. Wilson. 1972. Water resources of the Center Hill Lake region, Tennessee. Water Resources Series 9. Tennessee Department of Conservation, Division of Water Resources, Nashville, Tennessee.

Newcome, Roy, Jr., and Ollie Smith, Jr. 1962. Geology and ground-water resources of the Knox Dolomite in Middle Tennessee. Water Resources Series 4. Tennessee Department of Conservation and Commerce, Division of Water Resources, Nashville, Tennessee.

Reeves, Mark, and J. O. Duguid. 1975. Water movement through a saturated-unsaturated porous media: a finite-element Galerkin model. ORNL-4927.

Sinclair, A. J. 1976. Applications of probability graphs in mineral exploration. Special Vol. 4. Assoc. Explor. Geochem.

Sledz, J. J., and D. D. Huff. 1981. Computer model for determining fracture porosity and permeability in the Conasauga Group. ORNL/TM-7695.

Smith, E. D., and N. D. Vaughan. 1985. Experiences with aquifer testing and analysis in fractured low-permeability sedimentary rocks exhibiting nonradial pumping response. pp. 137-149. IN Hydrogeology of Rocks of Low Permeability. Memoirs of the 17th International Congress, International Association of Hydrogeologists, Part 1, Proceedings. Tucson, Arizona.

Snow, D. T. 1968. Rock fracture spacings, openings, and porosities. J. Soil Mech. Found. Div., Proc. Am. Soc. Civil Engrs. 94:73-91.

Snow, D. T. 1969. Anisotropic permeability of fractured media. Water Resour. Res. 5(6):1273-1289.

Stockdale, P. B. 1951. Geologic conditions at the Oak Ridge (X-10) area relevant to the disposal of radioactive waste. ORO-58. U.S. Atomic Energy Commission, Oak Ridge Operations, Oak Ridge, Tennessee.

Swank, W. T., and D. A. Crossley, Jr., eds. 1988. Forest hydrology and ecology at Coweeta [Hydrologic Laboratory, U.S. Forest Service, Otto, North Carolina]. Springer-Verlag, New York.

Tennessee Division of Water Resources. 1961. Tennessee's Water Resources. Tennessee Department of Conservation and Commerce, Nashville, Tennessee.

Tucci, Patrick. 1985. Ground-water flow in Melton Valley, Oak Ridge Reservation, Roane County, Tennessee--Preliminary model analysis. U.S. Geol. Surv. Water-Resour. Invest. Rep. 85-4221, Nashville, Tennessee.

U.S. Environmental Protection Agency. 1986. RCRA ground-water monitoring technical enforcement guidance document. OSWER-9950.1. U.S. Environmental Protection Agency, Washington, D.C.

Watson, K. W., and R. J. Luxmoore. 1986. Estimating macroporosity in a forest watershed by use of a tension infiltrometer. Soil Sci. Soc. Am. J. 50:578-582.

Webster, D. A. 1976. A review of hydrologic and geologic conditions related to radioactive solid-waste burial grounds at Oak Ridge National Laboratory, Tennessee. U.S. Geol. Surv. Open-File Rep. 76-727, Nashville, Tennessee.

Webster, D. A., and M. W. Bradley. 1987. Hydrology of the Melton Valley radioactive-waste burial grounds at Oak Ridge National Laboratory, Tennessee. U.S. Geol. Surv. Open-File Rep. 87-686, Nashville, Tennessee.

Wilson, G. V., and R. J. Luxmoore. 1988. Infiltration, macroporosity, and mesoporosity distributions on two forested watersheds. Soil Sci. Soc. Am. J. 52(2):329-335.

Witherspoon, P. A., J. S. Y. Wang, K. Iwai, and J. E. Gale. 1980. Validity of cubic law for fluid flow in a deformable rock fracture. Water Resour. Res. 16(6): 1016-1024.

Yeh, G. T. 1987. FEMWATER: a finite element model of water flow through saturated-unsaturated porous media, a first revision. ORNL-5567/R1.

Yeh. G. T. 1988. 1DFEMWATER: a one-dimensional finite element model of water flow through saturated-unsaturated media. ORNL-6423.

Yeh, G. T., and D. S. Ward. 1980. FEMWATER: a finite element model of water flow through saturated-unsaturated porous media. ORNL-5567.

INTERNAL DISTRIBUTION

1. T. L. Ashwood
2. L. D. Bates
3. J. B. Berry
4. B. A. Berven
5-8. W. J. Boegly, Jr.
9. H. E. Braunstein
10. T. W. Burwinkle
11. J. B. Cannon
12-26. R. B. Clapp
27. K. W. Cook
28. A. G. Croff
29. R. B. Dreier
30. S. P. DuMont
31. T. O. Early
32. N. D. Farrow
33. T. A. Fontaine
34. C. E. Frye
35. H. R. Gaddis
36. S. B. Garland
37. S. M. Gregory
38. R. D. Hatcher
39. S. G. Hildebrand
40-44. D. D. Huff
45. P. M. Jardine
46. C. M. Kendrick
47. R. H. Ketelle
48. E. H. Krieg, Jr.
49. L. C. Lasher
50. R. R. Lee
51. J. M. Loar
52. L. W. Long
53. R. J. Luxmoore
54. L. L. McCauley
55. W. M. McMaster
56. C. P. McGinnis
57. M. E. Mitchell
58-82. G. K. Moore
83. G. M. Morrissey
84. C. E. Nix
85. C. R. Olsen
86-87. P. T. Owen
88. T. A. Perry
89. D. E. Reichle
90. P. S. Rohwer
91. T. H. Row
92. T. F. Scanlan
93. R. J. Selfridge
94. E. D. Smith
95. B. P. Spalding
96. S. H. Stow
97. L. E. Stratton
98. J. Switek
99. L. E. Toran
100. J. R. Trabalka
101. R. R. Turner
102. S. D. Van Hoesen
103. W. Van Winkle
104. L. D. Voorhees
105. D. J. Wickliff
106. Central Research Library
107-121. ESD Library
121-122. Laboratory Records Dept.
123. Laboratory Records, ORNL-RC
124. ORNL Patent Section
125. ORNL Y-12 Technical Library

EXTERNAL DISTRIBUTION

126. V. Dean Adams, Director, Center for Management Utilization and Protection of Water Resources, Tennessee Technological University, Box 5082, Cookeville, TN 38501
127. R. P. Berube, Deputy Assistant Secretary for Environment, EH-20, U.S. Department of Energy, Washington, DC 20585
128. C. M. Borgstrom, Director, Office of NEPA Project Assistance, EH-25, U.S. Department of Energy, Washington, DC 20585
129. J. S. Brehm, Office of Surplus Facilities Management, UNC Nuclear Industries, P.O. Box 490, Richland, WA 99352

130. J. T. Callahan, Associate Director, Ecosystem Studies Program, Room 336, 1800 G Street, NW, National Science Foundation, Washington, DC 20550
131. T. C. Chee, R&D and Byproducts Division, DP-123 (GTN), U.S. Department of Energy, Washington, DC 20545
132. A. T. Clark, Jr., Advanced Fuel and Spent Fuel Licensing Branch, Division of Fuel Cycling and Material Safety, 396-SS, U.S. Nuclear Regulatory Commission, 7915 Eastern Avenue, Silver Spring, MD 20910
133. R. R. Colwell, Director, Maryland Biotechnology Institute, University of Maryland, Microbiology Bldg., College Park, MD 20742
134. E. F. Conti, Office of Nuclear Regulatory Research, Nuclear Regulatory Commission, MS-1130-SS, Washington, DC 20555
135. W. E. Cooper, Department of Zoology, College of Natural Sciences, Michigan State University, East Lansing, MI 48824
136. N. H. Cutshall, 10461 White Granite Dr., Suite 204, Oakton, VA 22124
137. J. E. Dieckhoner, Acting Director, Operations and Traffic Division, DP-122 (GTN), U.S. Department of Energy, Washington, DC 20545
138. J. Farley, Office of Energy Research, U.S. Department of Energy, ER-65, Washington, DC 20545
139. G. J. Foley, Director, Environmental Monitoring Systems Laboratory, MD-75, Research Triangle Park, NC 27711
140. B. J. Frederick, Department of Civil Engineering, The University of Tennessee, Knoxville, TN 37916
141. R. D. Glenn, Bechtel National Inc., P.O. Box 350, Oak Ridge, TN 37831-0350
142. C. R. Goldman, Professor of Limnology, Director of Tahoe Research Group, Division of Environmental Studies, University of California, Davis, CA 95616
143. W. F. Harris, Executive Office to the Assistant Director for Biological, Behavioral, and Social Sciences, National Science Foundation, Washington, DC, 20550
144. R. C. Harriss, National Aeronautics and Space Administration, Langley Research Laboratory, Hampton, VA 23665
145. E. F. Hollyday, USGS-WRD, 412 Federal Building, U.S. Courthouse, Nashville, TN 37203
146. B. S. Hood, Bechtel National Inc., P.O. Box 350, Oak Ridge, TN 37831-0350
147. G. H. Hornberger, Department of Environmental Sciences, Clark Hall, University of Virginia, Charlottesville, VA 22903
148. J. W. Huckabee, Manager, Ecological Studies Program, Electric Power Research Institute, 3412 Hillview Avenue, P.O. Box 10412, Palo Alto, CA 94303
149. E. A. Jordan, Office of Defense Programs, U.S. Department of Energy, DP-122, Washington, DC 20545
150. G. Y. Jordy, Director, Office of Program Analysis, Office of Energy Research, ER-30, G-226, U.S. Department of Energy, Washington, DC 20545
151. P. M. Kearl, Oak Ridge National Laboratory, Grand Junction Office, U.S. Department of Energy, P.O. Box 2567, Grand Junction, CO 28135

152. N. Korte, Oak Ridge National Laboratory, Grand Junction Office, U.S. Department of Energy, P.O. Box 2567, Grand Junction, CO 81502
153. D. B. Leclaire, Director, Office of Defense Waste and Transportation Management, DP-12 (GTN), U.S. Department of Energy, Washington, DC 20545
154. G. E. Likens, Director, The New York Botanical Garden, Institute of Ecosystem Studies, The Mary Flagler Cary Arboretum, Box AB, Millbrook, NY 12545
155. R. D. Livesay, USGS-WRD, 1013 N. Broadway, Knoxville, TN 37917
156. H. M. McCammon, Director, Ecological Research Division, Office of Health and Environmental Research, Office of Energy Research, ER-75, U.S. Department of Energy, Washington, DC 20545
157. C. E. Miller, Surplus Facilities Management Program Office, U.S. Department of Energy, Richland Operations, P.O. Box 550, Richland, WA 99352
158. W. E. Murphie, Office of Remedial Action and Waste Technology, U.S. Department of Energy, NE-23, Washington, DC 20545
159. E. O'Donnell, Division of Radiation Programs and Earth Sciences, U.S. Nuclear Regulatory Commission, Mail Stop 1130 SS, Washington, DC 20555
160. F. L. Parker, College of Engineering, Institute of Water Resources, Vanderbilt University, Nashville, TN 37325
161. F. Quinones, U.S. Department of Interior, Geological Survey, Water Resources Division, A-413 Federal Building, U.S. Courthouse, Nashville, TN 37203
162. G. Reed, Department of Civil Engineering, The University of Tennessee, Knoxville, TN 37916
163. Ilkka Savolainen, Waste Management Section, International Atomic Energy Agency, Wagramerstrasse 5, P.O. Box 100, A-1400 Vienna, Austria
164. C. B. Sherwood, 11418 Lowndesboro Drive, Jacksonville, FL 32223
165. D. K. Solomon, 104 Seagram Dr. #326, Waterloo, Ontario, Canada, N213B8
166. R. J. Starmer, HLW Technical Development Branch, Office of Nuclear Material Safety and Safeguards, Nuclear Regulatory Commission, Room 427-SS, Washington, DC 20555
167. Ken Walker, Department of Geology, The University of Tennessee, Knoxville, TN 37916
168. Raymond G. Wilhour, U.S. Environmental of Protection Agency, Environmental Research Laboratory, Sabine Island, Gulf Breeze, FL 32561
169. Frank J. Wobber, Ecological Research Division, Office of Health and Environmental Research, Office of Energy Research, ER-75, Department of Energy, Washington, DC 20545
170. J. G. Yates, Office of Energy Research, U.S. Department of Energy, ER-42, Washington, DC 20585
171. Office of Assistant Manager for Energy Research and Development, Oak Ridge Operations, P.O. Box 2001, U.S. Department of Energy, Oak Ridge, TN 37831

172-181. Office of Scientific and Technical Information, P.O. Box 62, Oak Ridge, TN 37831

☆U.S. GOVERNMENT PRINTING OFFICE:1990-748-11400148